The mid-Piacenzian of the North Atlantic Ocean

Harry J. Dowsett[1], Marci M. Robinson[1], Kevin M. Foley[1], Timothy D. Herbert[2], Bette L. Otto-Bliesner[3] and Whittney Spivey[1,4]

[1]*Florence Bascom Geoscience Center, U.S. Geological Survey, Reston, VA 20192*

[2]*Department of Earth, Environmental and Planetary Sciences, Brown University, Providence, RI 02912*

[3]*Climate and Global Dynamics Laboratory, National Center for Atmospheric Research, Boulder, CO 80307*

[4]*Department of Geological Sciences, East Carolina University, Greenville, NC 27858*

Corresponding author email: hdowsett@usgs.gov

ABSTRACT: The Piacenzian Age (Pliocene) represents a past climate interval within which frequency and magnitude of environmental changes during a period of past global warmth can be analyzed, climate models can be tested, and results can be placed in a context to better prepare for future change. Here we focus on the North Atlantic region, incorporating new and existing faunal assemblage and alkenone paleotemperature data from Ocean Drilling Program Sites 642, 662, 982, and 999, and International Ocean Discovery Program Sites 1308 and 1313 into our paleoenvironmental reconstruction. Cores and outcrop material containing Piacenzian sediments from the Atlantic Coastal Plain of Virginia, USA, are also included. These data allow us to characterize regional changes in temperature, salinity, upwelling, surface productivity, and diversity, associated with climate transitions, and make nuanced reconstructions of mid-Piacenzian conditions within a high-resolution temporal framework between ~3.40 and ~3.15 Ma, inclusive of Marine Isotope Stages M2 through KM5. We include an initial comparison of estimated sea-surface temperature to coupled climate model simulations, which shows improvement in model adherence to paleoclimate parameters over previous data-model comparisons for the Pliocene.

INTRODUCTION

With scientific consensus attributing Earth's unprecedented warming in large part to anthropogenic greenhouse gasses (IPCC 2013; Wuebbles et al. 2017) it is common practice to simulate potential future change states using climate models. These simulations can help to better establish baselines of natural climate variability and to bracket ranges of potential environmental impacts, which in turn can be used to inform policy decisions required for societal scale adaptation and remediation. Atmospheric CO_2 concentrations, considered by most in the scientific community to be the significant driver of global warming, have recently surpassed levels (410 ppmv) experienced during the course of human evolution. The last time Earth exhibited atmospheric CO_2 concentrations and a climate similar to what is projected for the end of this century and beyond was ~3 million years ago (Ma), during the Piacenzian Age of the Pliocene Epoch (Badger 2013). Intuitively, it makes sense that understanding the climate system and environmental conditions during the Piacenzian equilibrium climate could inform us, by analogy, of the frequency, magnitude and impacts of changes we might expect in the future. The Piacenzian becomes even more relevant if any one of the IPCC AR6 mitigation scenarios is adopted to limit continued future warming (Rogelj et al. 2018; Gidden et al. 2019).

In the late 1980's, the U.S. Geological Survey initiated "Pliocene Research, Interpretation and Synoptic Mapping" (PRISM) to better understand Pliocene climatic conditions, map its environments on land and sea, and provide the climate modelling community with an evolving set of boundary conditions including sea-surface temperature (SST), deep ocean temperature (DOT), sea-ice distribution, land-ice volume and distribution, sea level, topography, bathymetry, and distribution of land vegetation. PRISM, presently in its fourth phase, also develops comparison data in the form of SST, surface air temperature (SAT), and proxy precipitation data, to enable analysis of numerical modelling simulations of a past period of extended global warmth (Dowsett et al. 2016).

Global scale spatial reconstructions and syntheses of Pliocene conditions at specific temporal horizons (e.g., Zubakov and Borzenkova 1988; Dowsett et al. 1994; 2010; 2016; Thompson and Fleming 1996; Salzmann et al. 2008, 2013; Sohl et al. 2009) provide conceptual models of the Earth climate system as well as a source of boundary conditions for model simulations and comparison data for climate model experiments (Haywood et al. 2016a). The Pliocene Model Intercomparison Project (PlioMIP) used PRISM3 boundary conditions (Dowsett et al. 2010) and comparison data (Dowsett et al. 2012; 2013a; Salzmann et al. 2013) to contrast simulations from eight different models (Haywood et al. 2013b). PlioMIP contributed more than 50 publications to our understanding of the Pliocene climate system and identified three areas for possible improvement in research and modelling: 1) The temporal resolution of paleoenvironmental data used for verification of model simulations needed refinement (Dowsett et al. 2013a; Haywood et al. 2013b; 2016a). 2) The largest discord between PlioMIP simulations and the marine verification data, occurring in the mid-to-high latitude North Atlantic Ocean, needed to be addressed (Dowsett et al. 2012). 3) Other aspects of the paleoenvironment (besides site specific SST) needed to be quantified with greater confidence for informing climate model simulations (Dowsett et al. 2013b).

In light of these PlioMIP findings, the scope and purpose of this contribution is to provide a more temporally resolved regional

TABLE 1
PRISM4 localities, estimated and simulated SST anomalies.

Locality		642	662	982	999	1308	1313	DEQ 161-592
Latitude (°N)		67.22	-1.39	57.52	12.74	49.88	41.00	36.68
Longitude (°E)		2.93	-11.74	-15.87	-78.74	-24.24	-32.96	-76.78
NOAA Ext. Recon. V5 (1870-1899)	SST (°C)	7.7	25.3	10.7	27.6	13.3	18.6	20.6
PRISM4	SST (°C)	13.90	26.76	17.10	28.00*	17.08	21.06	26.22
Dowsett et al. 2019	ΔSST (°C)	6.20	1.46	6.40	0.40	3.78	2.46	5.62
	σ	0.43	0.47	0.50	0.11	0.46	0.70	0.52
	n	5	7	8	2	6	7	10
CCSM4 (BS)	ΔSST (°C)	2.09	0.67	2.19	0.7	2.53	1.81	1.01
Otto-Bliesner et al. 2017	σ	0.61	0.46	0.4	0.35	0.82	0.5	0.48
CCSM4 (BS + CAA)	ΔSST (°C)	0.69	0.68	2.01	0.81	4.04	1.91	0.81
Otto-Bliesner et al. 2017	σ	0.83	0.44	0.38	0.36	0.66	0.49	0.46
CCSM4 (PlioMIP1)	ΔSST (°C)	0.93	0.66	1.69	0.79	1.08	1.25	1.06
Rosenbloom et al. 2013	σ	0.69	0.45	0.39	0.36	0.72	0.48	0.49

*alkenone based SST estimate for Site 999 taken from compilation of Foley and Dowsett (2019).

reconstruction of the North Atlantic Ocean focusing on aspects of the environment that can be discerned by faunal and geochemical data. We document changes in species abundances, assemblage composition and diversity relative to the pre-industrial (PI) era, and tie these to independent estimates of environmental change like SST based upon analysis of biomarkers. These data can then be used to assess the performance of climate model simulations (Otto-Bliesner et al. 2017) as well as the next phase of Pliocene model intercomparison, PlioMIP2 (Haywood et al. 2016b).

CHRONOLOGY

PRISM3 time slab

Prior to the availability of a high-resolution oxygen isotope scheme as a chronological framework, PRISM used the average interglacial condition over a ~300 ky interval to correlate between sites (Dowsett and Poore 1991). This interval, referred to as the PRISM *time slab* or *mid-Pliocene warm period* (mPWP), was used for the PRISM2 reconstruction (Dowsett 2007). The PRISM time slab (text-fig. 1), consisting of an interval of warm and stable climate (relative to high-amplitude Pleistocene glacial-interglacial cycles) positioned within the Piacenzian Stage, was refined through improved chronological control using the LR04 time scale to span the time between the transition of marine isotope stages (MIS) M2/M1 (3.264 Ma; revised to ~3.28Ma, Ahn et al. 2017) and G21/G20 (3.025Ma) in the middle part of the Gauss normal polarity Chron (Dowsett et al. 2010; 2016). The interval covers ~250 kyr and ranges from C2An2r (Mammoth reversed polarity) to near the bottom of C2An1 (just above Kaena reversed polarity), correlating in part to planktonic foraminiferal zones PL3 (*Sphaeroidinellopsis seminulina* Highest Occurrence Zone), PL4 (*Dentoglobigerina altispira* Highest Occurrence Zone) and PL5 (*Globorotalia miocenica* Highest Occurrence Zone). Within the bounding positive $\delta^{18}O$ excursions that mark glacial stages M2 and G20, and excepting glacial stage KM2 at ~3.1 Ma, benthic foraminiferal oxygen isotope values in this interval are equal to or isotopically lighter than those measured today, making this interval relatively easy to distinguish. See Robinson et al. (2018) for additional information on the development of the PRISM time slab.

Changes to the International Stratigraphic Code led to redefinition of the base of the Pleistocene Epoch (Series) to be in the San Nicola GSSP of the Gelasian Age (Stage) (Gibbard et al. 2010). This reassignment of the Gelasian to the Pleistocene Epoch (Series), resulted in limiting the Pliocene to the Zanclean Age (Stage) and Piacenzian Age (Stage). Thus, "mid-Pliocene" has a very different meaning pre- and post-2010. To avoid confusion in the literature and still maintain correct stratigraphic terminology, we now correctly refer to this interval of time, previously labeled mid-Pliocene, as the *mid-Piacenzian warm period (mPWP)* (Dowsett et al. 2016).

PRISM4 time slice

With PlioMIP2 protocols requiring orbital scale resolution for comparison data, the time slab concept, as defined above, has been modified. PRISM4 uses shorter, higher resolution time-series aligned to the LR04 stack of Lisiecki and Raymo (2005) to resolve conditions at MIS KM5c (~3.205 Ma) (Dowsett et al. 2013b; Haywood et al. 2013a; 2016b; Prescott et al. 2014; text-figs. 1 and 2). Ages assigned to isotopic stages in LR04 may be incorrect in the Piacenzian by as much as ~15 kyr (Lisiecki and Raymo 2005; Ahn et al. 2017). The new probabilistic stack of benthic $\delta^{18}O$ (Ahn et al. 2017) provides increased understanding of the relative uncertainty of records within and those aligned to the LR04 stack. Along with other potential sources of chronological error, correlation of Pliocene deep-sea sequences in terms of absolute time, at suborbital scales, remains problematic. Thus, we caution against making too precise statements regarding sequencing of events from different regions of the North Atlantic. With this caveat in mind, all records used in this study have been correlated to LR04 and are assumed to be synchronous.

LOCALITIES

We use North Atlantic sites with adequate carbonate preservation and accumulation rates sufficient to allow alignment to the LR04 chronology: Ocean Drilling Program (ODP) Sites 642,

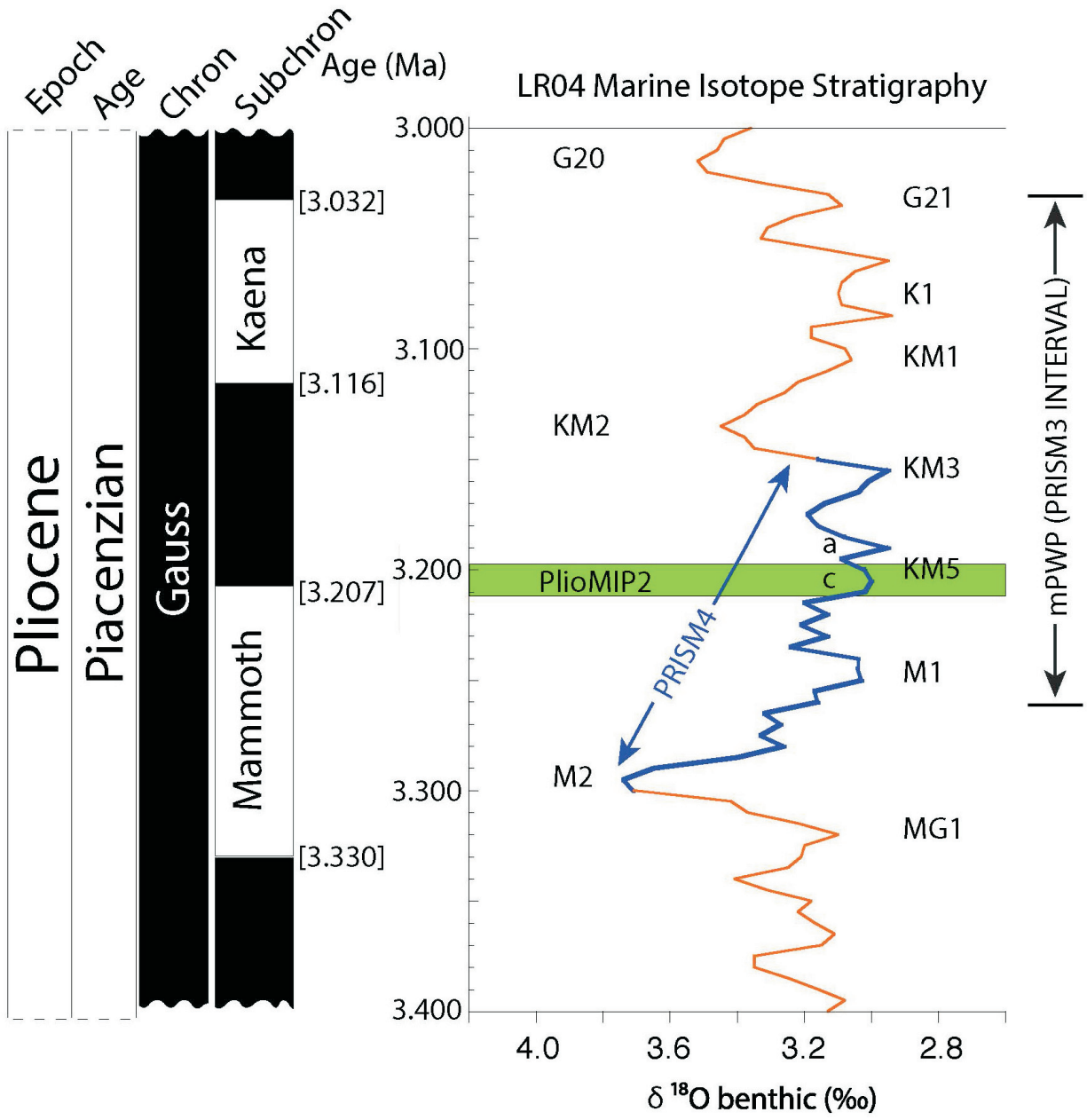

TEXT-FIGURE 1
Position of the mid-Piacenzian Warm Period (mPWP) PRISM3 interval, PRISM4 focus interval, and PlioMIP2 time slice, with respect to the geomagnetic polarity time scale (black normal, white reversed) showing bounding ages of Kaena and Mammoth reversals in brackets (Ogg et al. 2012), and LR04 benthic isotope stack (Lisiecki and Raymo 2005).

662, 982, 999 and International Ocean Discovery Program (IODP) Sites 1308, 1313 and Virginia Department of Environmental Quality (DEQ) Site 161-592 (Table 1; text-fig. 2). The Piacenzian intervals at these sites have been assigned a stratigraphic fidelity of *1a*, indicating better than 5000-year sampling resolution and orbital tuning (Dowsett et al. 2016).

ODP Site 642

Located at 67.23° N, 2.93° E in a water depth of 1286 m, Site 642 is the most northern locality considered in this reconstruction. Ages are determined from paleomagnetic reversals and a benthic oxygen isotope record (Risebrobakken et al. 2016). Alkenone SST (Bachem et al. 2016) and pollen records (Panitz et al. 2016) are available, and correlation of marine and terrestrial conditions for the mid-Piacenzian, along with accompanying data, are discussed in Panitz et al. (2018).

ODP Site 662

Located on the flank of the mid-Atlantic Ridge, in the eastern equatorial Atlantic (1.39° S, 11.73° W) in 3814 m of water, this is the most southern locality used in our reconstruction. The age model for Site 662 is based upon its benthic oxygen isotope re-

cord (Lisiecki and Raymo 2005). Alkenone based SST records are available (Herbert et al. 2010; Dowsett et al. 2017) and faunal abundance data have been developed as part of this paper (Robinson et al. 2019).

ODP Site 982

Located on the Rockall Plateau (57.52° N, 15.87° W) in 1134 m of water, Site 982 has an age model based upon revision of the original stratigraphy presented by the shipboard scientific party (Shipboard Scientific Party, 1996; Khelifi et al. 2012). Alkenone data are available from Lawrence et al. (2009), and new faunal and alkenone data were produced as part of the PRISM4 effort (Dowsett et al. 2017; Robinson et al. 2019).

ODP Site 999

This site is located in 2828 m of water on a bathymetric high within the Colombian Basin, Caribbean Sea (12.74° N, 78.74° W). We use the Site 999 age model created by Haug and Tiedemann (1998) and modified by Steph et al. (2006). We incorporate alkenone based SST (Badger et al. 2013; Dowsett et al. 2017) supplemented with faunal (Robinson et al. 2019) and Mg/Ca (O'Brien et al. 2014) estimates in our reconstruction.

IODP Site 1308

Situated on the eastern limb of the Mid-Atlantic Ridge (49.88° N, 24.24° W) at a water depth of 3900 m, this site has an age-model that utilizes planktonic foraminifer oxygen isotope data and paleomagnetic stratigraphy to align to the LR04 time scale (De Schepper et al. 2009). Planktonic foraminiferal assemblages (Robinson et al. 2019) and alkenone data (Dowsett et al. 2017) were extracted as part of this study.

IODP Site 1313

This site is a redrill of ODP Site 607, located in 3426 m of water on the western flank of the Mid-Atlantic Ridge (41.00° N, 32.96° W). The age model is based upon tuning the record of lightness (L*) to LR04 (Naafs et al. 2012). Alkenone data used in this study come from Naafs et al. (2012) supplemented by Dowsett et al. (2017). Planktonic foraminiferal assemblages were extracted as part of this study (Robinson et al. 2019).

Atlantic Coastal Plain DEQ 161-592 (Holland Core)

Located at 36.68° N, 76.78° W, in Holland, Virginia, USA, this site is approximately 45 km SSW of the lectostratotype of the Yorktown Formation at Rushmere, Virginia (Ward and Blackwelder 1980) and 75 km from the present-day Atlantic shoreline. Alkenone data were extracted for this study (Dowsett et al., 2017). DEQ 161-592 contains a well-preserved Yorktown sequence which includes the MIS M2 through KM5 interval (text-fig. 3).

A combination of biostratigraphic, paleomagnetic and for the first time, biomarker analyses, now provide a chronologic framework for the Yorktown Formation that agrees with previous attempts to place it within the deep-sea oxygen isotope stratigraphy (Krantz 1991; Ward et al. 1991) (text-fig. 3). The Yorktown Formation is an unconformity bounded package of fine-grained sandy clays and shell marls subdivided into a basal Sunken Meadows Member (equivalent to Zone 1 of Mansfield 1943) unconformably overlain by the Rushmere, Morgarts Beach and Moore House Members, which are collectively equivalent to Zone 2 of Mansfield (1943) (Ward and Blackwelder 1980) (text-fig. 3A). The Rushmere Member represents a rapid transgression and conformably grades into the overlying finer grained Morgarts Beach Member. A brief hiatus and disconformity separate the Morgarts Beach Member from the overlying Moore House Member. Zone 1 Yorktown is assigned to the Zanclean and Zone 2 the Piacenzian, using mollusks, foraminifers and ostracodes (Ward and Blackwelder 1980; Dowsett and Wiggs 1992; Hazel 1971). The Yorktown Formation rests unconformably on Miocene sediments belonging to the Eastover Formation and is unconformably overlain by the Chowan River Formation or other Pleistocene units.

Limited and equivocal data have until now allowed for only a general age determination primarily based upon planktonic foraminiferal and ostracod faunas from localities in southeastern Virginia and northeastern North Carolina (Hazel 1971; Snyder et al. 1983; Gibson 1983; Cronin et al. 1989; Dowsett and Wiggs 1992). Planktic foraminiferal data consistent with a zonal assignment of N19 (Blow 1969) or PLlb- PL3 (Berggren 1973) along with the presence of *Globorotalia puncticulata* (first appearance in the northern mid-latitudes ~4.1-3.9 Ma) and *Dentoglobigerina altispira* (last appearance ~2.9 Ma) in many Yorktown samples, suggest an age range of 4.0-2.9 Ma for the Yorktown Formation in the type area (Dowsett and Wiggs 1992).

Unpublished paleomagnetic analysis of the Chowan River Formation at the Yadkin Pit gives a reversed magnetic signal which together with biostratigraphic data suggests an early Matuyama age (Cronin et al. 1989). Another reversed interval is present at Yadkin Pit within the Morgarts Beach Member, below the unconformity separating the Yorktown from the overlying Pleistocene Chowan River Formation (Joseph E. Liddicoat; written communication 1981). This reversed interval could correlate to either the Kaena or Mammoth subchrons.

Within the Holland Core, the marine regression corresponding to the M2 glacial event eroded all Zanclean as well as latest Messinian aged material. Rushmere sediments assignable to the Piacenzian begin at the unconformity at 150.6' (45.90 m) and conformably grade into Morgarts Beach lithology by 145' (44 m) (text-fig. 3B). Immediately below the unconformity at 150.6' (45.90 m) sediments of the Eastover Formation are assigned to Miocene dinoflagellate zone DN10 of De Verteuil and Norris (1996). The occurrence of the dinoflagellate species *Invertocysta lacrymosa* at 33.7' (10.27 m) suggests an age for the uppermost Morgarts Beach sediments ≥ 2.74 Ma based upon De Schepper et al. (2009).

We use alkenone data extracted from U.S. Atlantic Coastal Plain sediments (Dowsett et al. 2017) to refine the Yorktown Formation age model. Paleontological data and stratigraphic relationships observed in the field allow the U^{k}_{37}SST record at DEQ 161-592 to be correlated to the record at IODP Site U1313 (Fig. 3B), and ultimately to the LR04 timescale of Lisiecki and Raymo (2005). This correlation places the M2/M1 transition (~3.30 Ma to ~3.24 Ma) as extending from the unconformity at the base of the transgressive Rushmere Member (150.6') up into the Morgarts Beach Member. The reversed interval at Yadkin Pit therefore must be assigned to the Kaena subchron (3.116 Ma – 3.032 Ma). This correlation indicates an average accumulation rate of ~2.14 cm•ky $^{-1}$ and places the KM5c interval between 110 and 100 feet (33.5 and 30.5 m respectively) within the lower part of the Morgarts Beach Member.

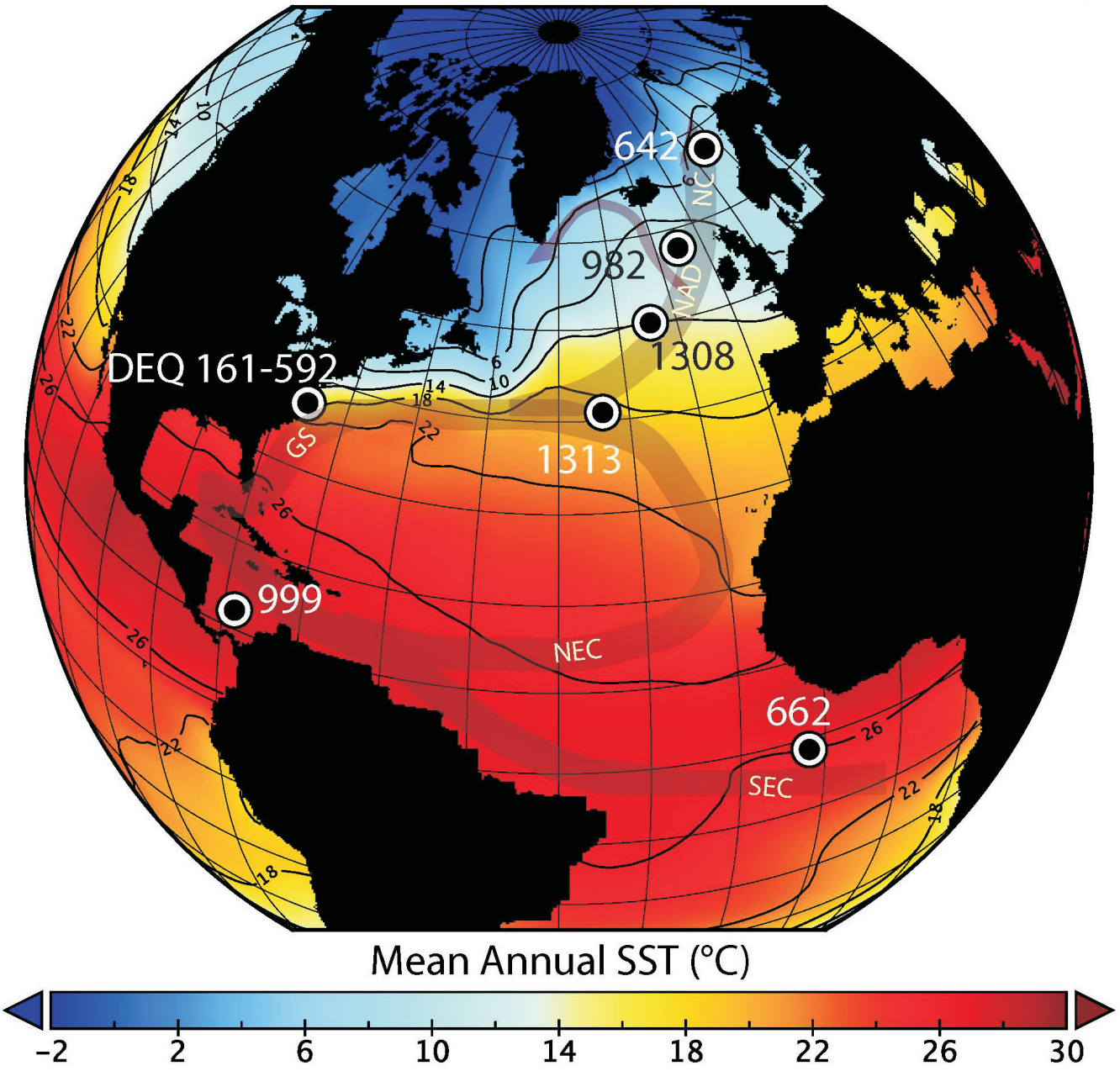

TEXT-FIGURE 2
PRISM4 localities projected on a pre-industrial (1870-1899 AD) mean annual sea surface temperature (SST) field (NOAA ERSSTv5, Huang et al. 2017). Primary elements of a simplified present day North Atlantic circulation are shown: GS- Gulf Stream, NAD- North Atlantic Drift, NC- Norwegian Current, NEC- North Equatorial Current, SEC- South Equatorial Current.

METHODS

Samples used in this study were analyzed using a combination of faunal methods and the alkenone index for estimating paleotemperature.

Alkenones

Alkenone paleothermometry (or the calibrated $U^{k'}_{37}$ index) is based upon the temperature dependence of double and triple carbon bonds in the alkenones produced by haptophyte algae (Volkman 2000; Herbert 2001, 2004; Lawrence et al. 2007). Temperature estimates derived using this technique have an analytical error of 0.1° C, are calibrated using the Müller et al. (1998) coretop calibration, and have a calibration uncertainty of ±1.38° C (Lawrence et al. 2007). Here we incorporate previously published alkenone data (Herbert et al. 2010; Lawrence et al. 2009; Khelifi et al. 2012; Naafs et al. 2010; Bachem et al. 2016, Badger et al. 2013) with new alkenone analyses from Sites 982, 999, 1308, 1313 and DEQ161-592 (Dowsett et al. 2017). Sediment samples of 1-5 g dry weight are extracted via a Dionex ASE (methylene chloride as solvent) and prepared for gas chromatography using toluene as the solvent for sample injec-

tion. Gas chromatographic analyses are carried out on Agilent 5890 and 6890 gas chromatographs equipped with 60 m DB-1 chromatographic columns and Flame Ionization Detection, with a temperature ramp at 25° C to 240° C, followed by ramping at 1.5° C to 320° C. Gas chromatographic quality control is maintained by daily analysis of a laboratory standard alkenone mixture, and by running the same sample at the beginning and end of each gas chromatograph run to determine sample drift due to changing chromatographic conditions. Analysis of both lab standard and sample replication indicates a long-term replication of U^k_{37} values equivalent to 0.1-0.2° C.

Planktonic foraminifera

Abundance data were obtained by processing sediment samples to extract and concentrate foraminifera. Samples are dried at ≤ 50° C, then agitated in a dilute solution (5 gL^{-1} water) of sodium hexametaphosphate solution for up to 2 hours. Samples are wet-sieved on a 63 µm mesh until clean, dried at ≤50° C, and then dry-sieved to concentrate the ≥150 µm coarse fraction. The coarse fraction is mechanically split to obtain, whenever possible, ~300 individual planktonic foraminifera specimens. Faunal slides are prepared by sorting into 64 taxonomic categories and fixed to 60-cell micropaleontological slides using a weak, water–soluble adhesive (polyvinyl acetate), following taxonomic concepts of Parker (1962; 1967), Blow (1969) and Dowsett and Robinson (2007).

For this study, approximately 58,000 specimens were identified and assigned to 45 species (Robinson et al. 2019). Species richness (*S*) and Shannon Diversity (*H'*) were calculated for all planktonic foraminifer bearing samples using

$$H' = -\sum_{i=1}^{s} p_i \ln p_i$$

where *S* is the total number of species and p_i the proportion of *S* made up of the *i*th species (Shannon 1948; Colwell 2013). We use generalized eco-groupings of Aze et al. (2011) and relative abundance of key taxa based upon an understanding of modern ecological preferences to investigate qualitative changes to mixed layer depth (MLD) and productivity (Bé 1977; Hemleben et al. 1989; Ravelo et al. 1990; Dowsett 1991; Chen 1994; see Supplement). Relative abundance of herbivores and taxa associated with upwelling regimes can be used to approximate primary productivity (e.g. Ivanova et al. 2012). Where possible, these estimates can be compared to the total C_{37} alkenone content of sediment samples, a proxy for total phytoplankton flux (Bolton et al. 2010).

Faunal slides and additional washed residue are archived at the U.S. Geological Survey's Florence Bascom Geoscience Center (FBGC) Foram Lab in Reston, Virginia, USA. Relative abundance of foraminiferal species is shown graphically in text-figure 4, and abundance data can be accessed at https://www.ncdc.noaa.gov/paleo/study/27310.

Assemblage analysis

We use *q*-mode factor analysis to resolve core-top (Modern) North Atlantic planktonic foraminiferal abundances (from the Brown University Foraminiferal Database; Prell et al. 1999) into five end-member assemblages. This process is summarized

$$U_M = B_M F$$

with U_M representing the normalized modern foraminiferal census, B_M the varimax (loadings) matrix providing the contribution of each assemblage to the Modern samples, and *F*, the factor description (scores) matrix which describes the composition of the Modern assemblages. Pliocene assemblages are then described as relative contributions from the five Modern assemblages of the North Atlantic model using the procedure originally outlined by Imbrie and Kipp (1971)

$$B_p = U_p F'$$

where B_p, the down-core Pliocene assemblages are obtained by post-multiplying the normalized Pliocene abundance data U_p by *F'*, the factor description (score) matrix from the core-top model. To assesses how well the core-top model explains the Pliocene data we calculate communality (h^2)

$$h_k^2 = \sum_{i=1}^{n} s_k^2$$

for each Pliocene sample (*k*) as the summation of the square of the factor loading (*s*) for factors *i* through *n*. Low communalities can be interpreted as possible indications of pre- and post-depositional dissolution, reworking, advection, evolution, taxonomic drift or changing ecological tolerances, all of which can contribute to non-analog assemblages.

Using the above method to establish assemblage composition in Pliocene faunas requires the additional step of assigning now extinct taxa, as well as extant taxa having evolved since the Piacenzian, to modern functional groups. The assumption of stationarity involved in this step precludes us from using a calibrated transfer function to estimate Pliocene temperatures, with two exceptions. We use transfer function GSF18 (see Dowsett and Poore 1990; Dowsett 2007) to supplement our limited alkenone-based SST estimates at Site 999, and also to estimate directional-changes in seasonality using the difference between warm-season (SSTw) and cold-season (SSTc) faunal-based temperatures (see Supplement).

RESULTS

Sea-Surface Temperature

SST estimates based upon the $U^{k'}_{37}$paleothermometer are shown for Sites 642, 662, 982, 999, 1308, 1313 and DEQ161-592 in text-figure 5. The overall latitudinal pattern of SST between sites is similar to present day. Sites 642 and 982 in the higher latitudes exhibit the coolest conditions, and Sites 999 and 662 in the lower latitudes show the warmest. Note that while the average unsaturation value obtained at Site 999 is quite high (0.971), no samples showed complete saturation that would indicate a truncation of the alkenone temperature response. Sites 982, 1308 and 1313 maintain the modern temperature ranking though at times merge to form a relatively gentle thermal gradient (e.g. during M2 glacial). Similarly, Hodell and Channell (2016) found the SST gradient between Sites 1313 and 982 was greatly reduced during Pleistocene glacials, relative to a 5° C interglacial gradient. The PI gradient between these sites is ~8° C (text-fig. 5). During the Piacenzian, except possibly during MIS KM5 and M2, the mean annual temperature gradient between these two sites rarely exceeds 2.5° C.

Most records (Sites 982, 1308, 1313, 662 and 999) show a recognizable cool peak associated with MIS M2. The most likely reason for the absence of extreme cooling at Site 642 during MIS M2 (3.312 to 3.264 Ma) is the presence of an undetected hiatus (Bachem et al. 2016). Site DEQ161-592 contains sediments representing the rapid transgression following the

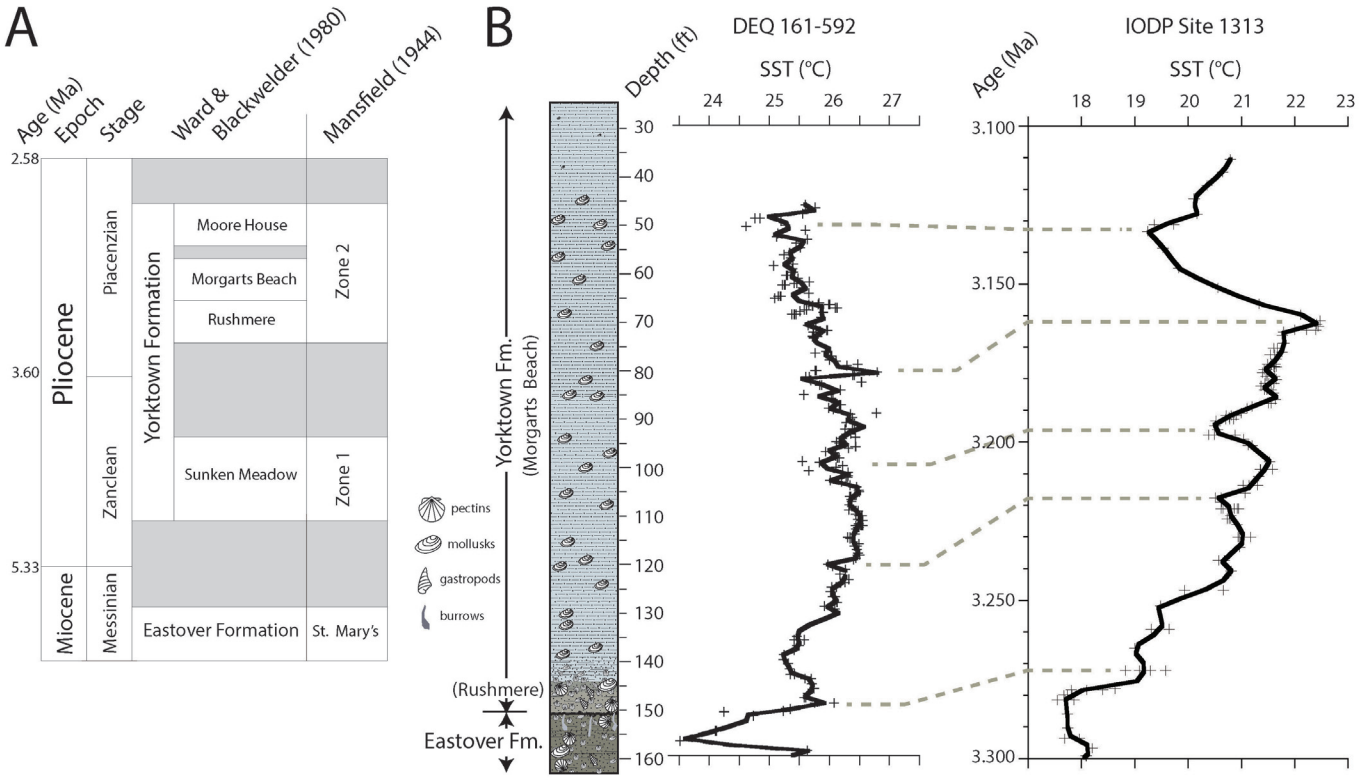

TEXT-FIGURE 3
A: Correlation chart and summary of stratigraphic terminology and temporal distribution of the Yorktown Formation and Members in southeastern Virginia. Ages of Stage boundaries from Ogg et al. (2012). B: Lithology of core DEQ 161-592 and correlation of alkenone sea surface temperature (SST) record to that of IODP Site 1313 (Naafs et al. 2012).

low-stand associated with MIS M2, and the M2/M1 transition, though sediments were either not preserved or not deposited during the peak M2 low-stand at this shallow marine site.

The amplitude of SST variability is highest in the mid-latitudes and dampened toward the equator. The magnitude of glacial – interglacial change at most sites is reduced compared to Pleistocene records (Kandiano et al. 2004). During MIS KM5c (~3.205 Ma), SST was higher than during the PI at all North Atlantic sites (text-fig. 5). At Site 999 we have a low resolution alkenone record which is a combination of estimates from Badger et al. (2013) and Dowsett et al. (2017). Subsequent to the M2 glacial event we plot a higher resolution faunal-based SST record (text-fig. 5). PRISM3 faunal-based mean annual SST estimates are generally cooler than alkenone-based estimates (e.g., Robinson et al. 2008; Tzanova and Herbert 2015; Herbert et al. 2015) and at Site 999 may be masking a positive temperature anomaly. Mg/Ca based estimates of Pliocene SST at Site 999, corrected for Mg/Ca of seawater, suggest Caribbean SST was warmer than faunal estimates, in close agreement with the alkenone estimates shown in text-figure 5 (O'Brien et al. 2014). Alkenone data from Badger et al. (2013) suggest a KM5c anomaly of +0.4°C (see also Foley and Dowsett 2019).

Peak cooling at MIS M2 shows minor changes in both structure and position. While differences in structure are undoubtedly documenting local conditions, offsets in the timing of peak cooling are somewhat problematic. Uncertainty in age-models and sample aliasing are most likely responsible for small differences between sites. Alternatively, though unlikely due to the small distances between sites, shifts in position could be interpreted as a phased temperature response.

Low-latitude sites (662 and 999) and Site 1313 show peak M2 temperatures slightly cooler than PI conditions. At mid to high latitude Sites (1308, 982, 642), cool conditions associated with M2 were still warmer than the PI values at those locations (text-fig. 5).

The KM5c event cannot be distinguished based upon relative temperature changes; identification is entirely dependent upon chronology. At low latitudes and along the east coast of North America (represented here by the Yorktown Formation), SST shows high frequency variability through the Piacenzian. Mean conditions at Site 662 and 999 are slightly warmer than PI conditions (text-fig. 5). The DEQ161-592 SST record also shows high-frequency, low-amplitude variability throughout the post-M2 interval, but the record is displaced by approximately +5 °C from PI conditions. Foraminifer, ostracode and mollusk faunas all show migration to positions farther north along the Atlantic Coastal Plain than at present, supporting an increase in both surface and shallow bottom water temperature possibly associated with a northward displacement of the gyre along the western Atlantic at this time (e.g., Cronin and Dowsett 1996; Saupe et al. 2014). Sites 1313, 1308, 982 and 642 show an increasing mean annual SST anomaly with increasing latitude (Table 1) (text-fig. 5).

Planktonic Foraminifera

Abundance and Variability

Relative abundances of planktonic foraminifer species at each site are shown in text-figure 4 (see also Robinson et al. 2019). The planktonic foraminiferal assemblages in the Piacenzian interval of the PRISM4 North Atlantic cores are quantitatively dominated by six taxa: *Globorotalia puncticulata, Globigerina bulloides, Neogloboquadrina incompta, Neogloboquadrina atlantica, Globigerinoides sacculifer* and *Globigerinita glutinata*. *Globorotalia puncticulata* is present in the three extratropical sites but is a minor constituent of assemblages from the two low latitude sites. There are an additional 22 taxa that have maximum occurrences between 10% and 25% in at least one sample. The remaining 16 taxa (text-fig. 4) are minor constituents of the assemblages.

Planktonic foraminifera distributions are controlled by a complex array of factors and changes in relative abundance of individual taxa and groups of taxa can provide useful paleoenvironmental information on salinity, productivity, and water column structure, in addition to SST. For example, *Globigerinoides sacculifer* occurs in greatest abundance in the Caribbean Sea (Site 999) with minor occurrences at equatorial Site 662 (text-fig. 4). Variability in the relative abundance of *Gs. sacculifer* (a stenohaline taxon) can be used at Site 999 to monitor the less-saline waters of the eastern Pacific entering the Caribbean Sea during temporary breaches of the Central American Isthmus (CAI) and warmer, more saline conditions building up when the Central American Seaway (CAS) was closed.

Both Sites 999 and 662 have tropical faunas characterized by *Dentoglobigerina altispira, Neogloboquadrina dutertrei, Globigerinoides ruber, Globorotalia menardii, Globigerinoides obliquus, Globigerina decoraperta, Neogloboquadrina acostaensis* and *Globigerina woodi*. High abundances of *N. dutertrei* in these two low latitude sites is suggestive of high productivity.

At Site 982 the faunal succession shows a change from cold elements to warmer transitional elements following peak M2 conditions: *Neogloboquadrina pachyderma* decreases in abundance as *G. bulloides* first increases and then decreases, giving way to *Gl. puncticulata* (text-fig. 4). The temporary absence (or sporadic very low abundance) of *Gl. puncticulata* in the North Atlantic during part of the Pliocene has been documented by previous workers (e.g., Loubere and Moss 1986; Weaver 1986; Dowsett and Poore 1990). The reappearance of this taxon in the North Atlantic occurs during warming associated with the M2/M1 transition. Ensuing glacial stages are marked by brief increases in *N. pachyderma* and sinistrally coiled *N. atlantica* (text-fig. 4). At Site 1308 a similar succession can be found showing repeated replacement of cooler faunas dominated by *N. incompta* by those with abundant *Gl. puncticulata*, indicating a change to warmer conditions. Farther south at Site 1313, just south of the present-day northern limb of the subtropical gyre, a similar transition is observed with *N. incompta* decreasing abundance following the peak of MIS M2, *Gl. puncticulata* becoming dominant as warmer waters are shifted north, followed by increased abundances of *Gl. crassaformis*. While present at all sites, *Gl. crassaformis* increases in abundance after M2 at Sites 982, 1308 and 1313. *Globorotalia crassaformis* prefers warm subtropical conditions and is generally considered a thermocline dweller, an occurrence pattern that fits well with the estimated warmth associated with isotope stages M1, KM5 and KM3 (text-fig. 4). In contrast, *Globorotalia hirsuta*, also a warm subtropical thermocline taxon with an average living depth ~170 m (Rebotim et al. 2017), reaches maximum abundance in the earlier part of MIS M2 through MIS KM5 and is most abundant at Site 1313. Thus, superimposed on warming documented by inclusion of subtropical elements farther north, the abundance pattern of *Gl. hirsuta,* followed by *Gl. crassaformis*, may reflect an overall change in mixed layer depth (MLD) from a deeper MLD with lower vertical water column gradients typical of cooler climates to one with a more pronounced thermocline as found in tropical areas (Hilbrecht 1996). Faunal productivity at Sites 1308 and 1313, indicated by increased abundances of *G. bulloides* and *Gl. puncticulata*, shows maxima at M2 and KM6 with concomitant increases in total C_{37} (Naafs et al. 2012). At both Sites 1313 and 1308, the transitional fauna generally increases as the North Atlantic Drift shifts farther north through MIS KM5, though alkenone based SST shows a more pronounced warming at Site 1313 than at 1308.

Neogloboquadrina acostaensis is more abundant at equatorial Atlantic Site 662 than at any of the other sites investigated. In addition, *N. acostaensis, Gt. glutinata and G. bulloides* all have abundance maxima at Site 662 coinciding with the SST cold peak at MIS M2. During a multiproxy reevaluation of Pliocene SST's in the North Atlantic, Robinson et al. (2008) interpreted high abundances of *N. acostaensis* as a probable indicator of productivity rather than temperature. Likewise, we interpret the increased relative abundances of these three taxa at 662 to track productivity consistent with higher relative productivity at MIS M2.

Neogloboquadrina atlantica, N. pachyderma and *Turborotalita quinqueloba*, all cold-water indicators, comprise the majority of the faunal assemblages at Site 982. Dowsett and Poore (1990) considered sinistrally coiled *N. atlantica* to be the cold end-member of the genus *Neogloboquadrina* during the Piacenzian due to its distribution at mid to high latitudes. At Site 982 positive $\delta^{18}O$ excursions and cold SST estimates correspond to increases in the relative abundance of *N. atlantica* as well as *N. pachyderma*. Variations in *G. bulloides* appear to be responses to productivity rather than to surface temperature. While not investigated as part of this study, the Piacenzian faunas at Site 642 are also dominated by sinistrally coiled *N. atlantica* and *G. bulloides* (Spiegler and Jansen 1989; unpublished data from Hole 642C).

DISCUSSION

North Atlantic Paleoceanography

Productivity and water column structure

Changes in the numbers of mixed layer, thermocline and sub-thermocline taxa may provide indications of relative change in MLD (text-fig. 6). We assume deepening of the mixed layer depth would introduce more nutrients to the mixed layer, thus increasing primary productivity. This is reflected in greater relative abundance of mixed layer (surface) planktonic foraminifers. Conversely, a decrease in MLD would result in decreased surface productivity and lead to greater relative abundance of thermocline (intermediate depth) taxa.

At Site 999 the overall decrease in mixed layer taxa and increase in thermocline taxa between M2 and KM5 suggests long

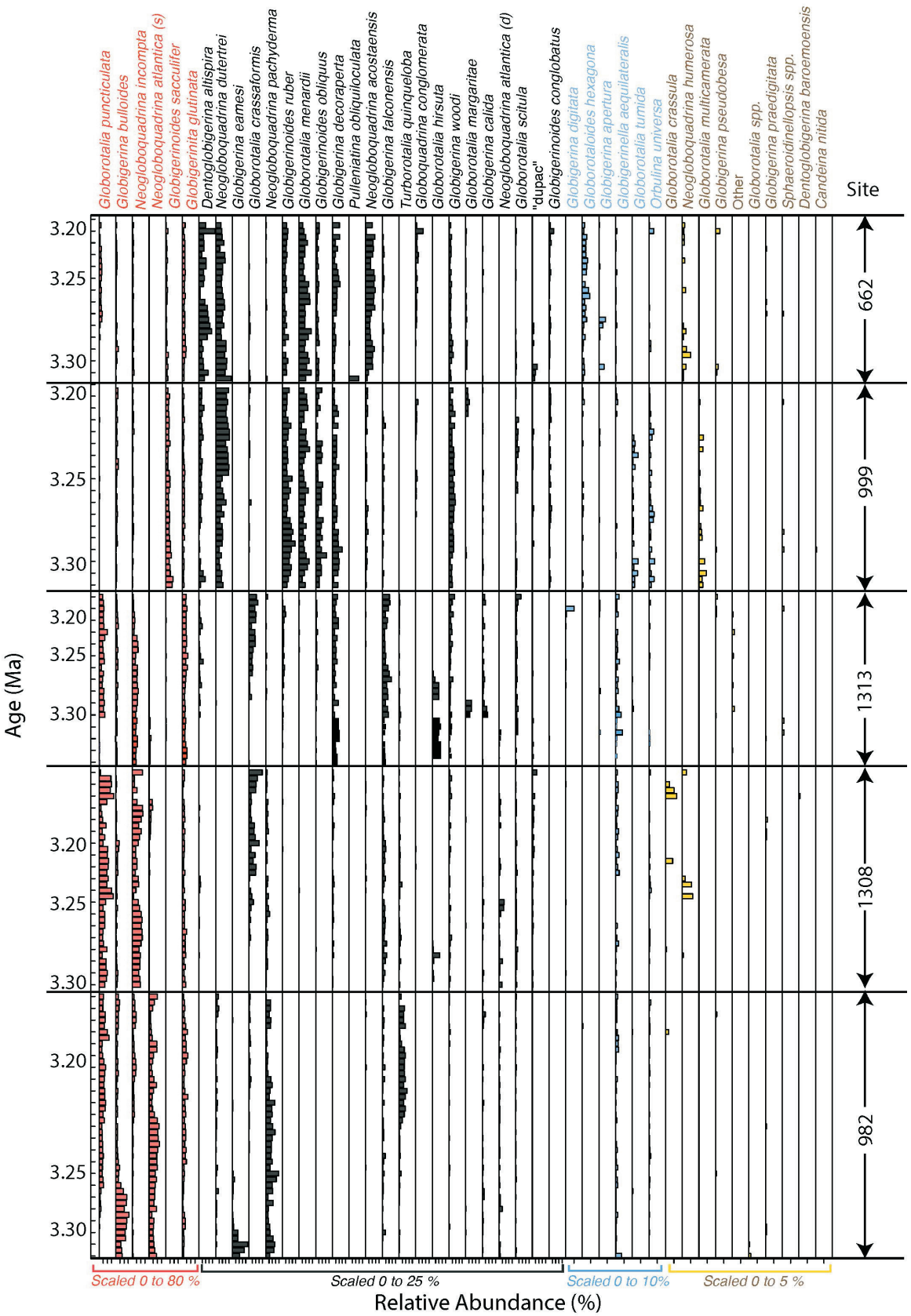

TEXT-FIGURE 4
Planktonic foraminifer relative abundances by age across five North Atlantic sites.
See Robinson et al. 2019 (https://www.ncdc.noaa.gov/paleo/study/27310) for census data.

term shoaling of the MLD and a more stratified water column (text-fig. 6). Superimposed on this trend are periodic changes in abundance from taxa associated with productivity (*Globigerina bulloides* and *Neogloboquadrina dutertrei*). We interpret these changes in relative faunal abundance to indicate periods of increased upwelling, nutrients, and productivity, combined with overall increasing salinity.

At Site 982 there is also a decrease in the abundance of mixed layer taxa between M2 and KM5, but this corresponds to replacement of the subpolar taxa by elements of the high latitude assemblage (i.e. *Neogloboquadrina incompta*, *Globigerinita glutinata*, and *Turborotalita quinqueloba*) that were not included in the categories plotted on text-figure 6, not a change in water column structure.

The M2 – M1 transition at Site 662 is characterized by an increase in mixed layer dwellers and concomitant decrease in thermocline dwellers (text-fig. 6). This suggests a change to a deeper mixed layer and less stratified water column. From M1 to KM6 this trend is reversed.

Diversity

Our faunal data allow comparison of latitudinal diversity gradients at several intervals within the Piacenzian. Average planktonic foraminifer diversity is greater in the tropics than at higher latitudes during the late Pliocene (text-fig. 6), and the relationship between planktonic foraminiferal diversity and temperature in the North Atlantic is constant over the past three million years (Yasuhara et al. 2012). Text-figure 6 shows the overall latitudinal gradient is maintained except possibly between 3.25 Ma and 3.20 Ma, when diversity at Sites 982, 1308 and 1313 converge. The fauna at Sites 662, 999, 1308 and 982 show an overall trend toward increasing diversity parallel to the environmental changes occurring between 3.30 and 3.15 Ma. High frequency variability in diversity is present at all sites, but higher amplitude changes occur at higher latitudes. Aside from Site 662, at all sites the MIS M2/M1 transition, considered the first major deglacial within the late Pliocene, is accompanied by an increase in species diversity. While diversity is higher in the tropics, when integrated over the entire study interval, Sites 1308 and 1313 exhibit higher species richness than either of the two tropical sites. We interpret this to be another indication of a highly variable Gulf Stream over this time interval, resulting in these sites recording a wider range of assemblages, and therefore high species richness values.

Assemblage analysis

Analysis of the North Atlantic core-top data yields 5 assemblages that together explain 95% of the variance in the fauna (Dowsett 2007). In this paper we combine our understanding of these original North Atlantic Pliocene planktonic foraminifer assemblages (Dowsett and Poore 1990) with those from Dowsett and Robinson (2007) and characterize the modern and Pliocene faunas as tropical, transitional, subpolar, high-latitude and gyre-margin (text-fig. 7). The boundary between tropical and transitional assemblages is approximately equivalent to the low latitude (LL) – mid-latitude (ML) boundary of Dowsett and Robinson (2007). Their high latitude (HL) assemblage coincides with the high-latitude and subpolar assemblages and overlaps with the northern part of the transitional assemblage shown in text-figure 7.

Text-figure 6 shows the relative strength of each of the 5 assemblages identified in text-figure 7 for each PRISM4 North Atlantic site. The Pliocene faunas at Sites 662 and 999 are dominated by both the tropical and the gyre-margin assemblages. In the Caribbean (Site 999), between M2 and KM5, there is an overall trend toward increasing importance of the gyre-margin assemblage at the expense of the tropical assemblage. If variations within the gyre-margin assemblage are interpreted as changes in productivity, the data suggest a high frequency inverse relationship between the two assemblages superimposed on an overall increase in productivity from M2 through KM5. At a finer scale, the M2/M1 transition is characterized by an increase in tropical assemblage taxa, which corresponds to warming at both sites. The relatively low abundance of the gyre margin fauna at Site 999 during MIS M2 may be due to a decreased inflow of nutrient-rich Pacific waters via the shoaling CAS.

Sites 1313, 1308 and 982 form a transect starting near the southern edge of the northern limb of the North Atlantic Gyre near the Azores, across the North Atlantic Drift to the Rockall Plateau (text-fig. 7). All three sites are dominated by the high-latitude and transitional assemblages which show an inverse relationship, with high amounts of transitional forms associated with KM5, although not as pronounced at Site 982 (text-fig. 6). At all three Sites the M2/M1 transition is marked by an increase in transitional taxa. Sites 1308 and 982 are dominated by the high latitude assemblage except for incursions of transitional elements during KM5.

Taken as a whole, the shifts in assemblages documented in text-figure 6 are evidence of an intermittent connection between the Atlantic and Pacific via the CAS, along with a Gulf Stream North Atlantic Drift system that migrated northward over the M2/M1 transition, exhibited high–frequency migrations north and south during M1 and KM6, and attained its most northern position by KM5. Over this same interval, pollen data at Site 642 show a migration of a deciduous to mixed forest to northern Norway, indicating terrestrial warming to greater than PI conditions (Panitz et al. 2016).

Chronostratigraphic Correlation of Records

A sound stratigraphic framework is the foundation of any paleoenvironmental reconstruction. Accurate determination of a single point in time in a marine sediment core is complicated by low and/or varying accumulation rates and bioturbation or other sediment disturbance that can distort or disguise the temporal signal. Accumulation rates vary geographically and temporally, but in the deep-sea sites discussed here generally range between 2 cm•ky^{-1} and 20 cm•ky^{-1}. Hence, a typical 1 cm sediment sample at best represents between 50 and 500 years. The paleoenvironmental estimate extracted from each sample, assuming accumulation rate was constant over those years, represents average conditions for that period of time. More likely, regional phytoplankton blooms and zooplankton patchiness result in uneven temporal and spatial fluxes. Bioturbation, likely to some degree in most marine sediments, further compromises sediment chronology by creating mixing, both upward and downward in the sediment column, shifting signal carriers from their original levels. In terms of isotopic or temperature signals, bioturbation can result in amplitude suppression or translational offset, adding uncertainty to any stratigraphic correlation. In records with lower sediment accumulation rates, signal mixing is exaggerated. The temporal signal can be further affected by post-depositional changes such as differential transport or ero-

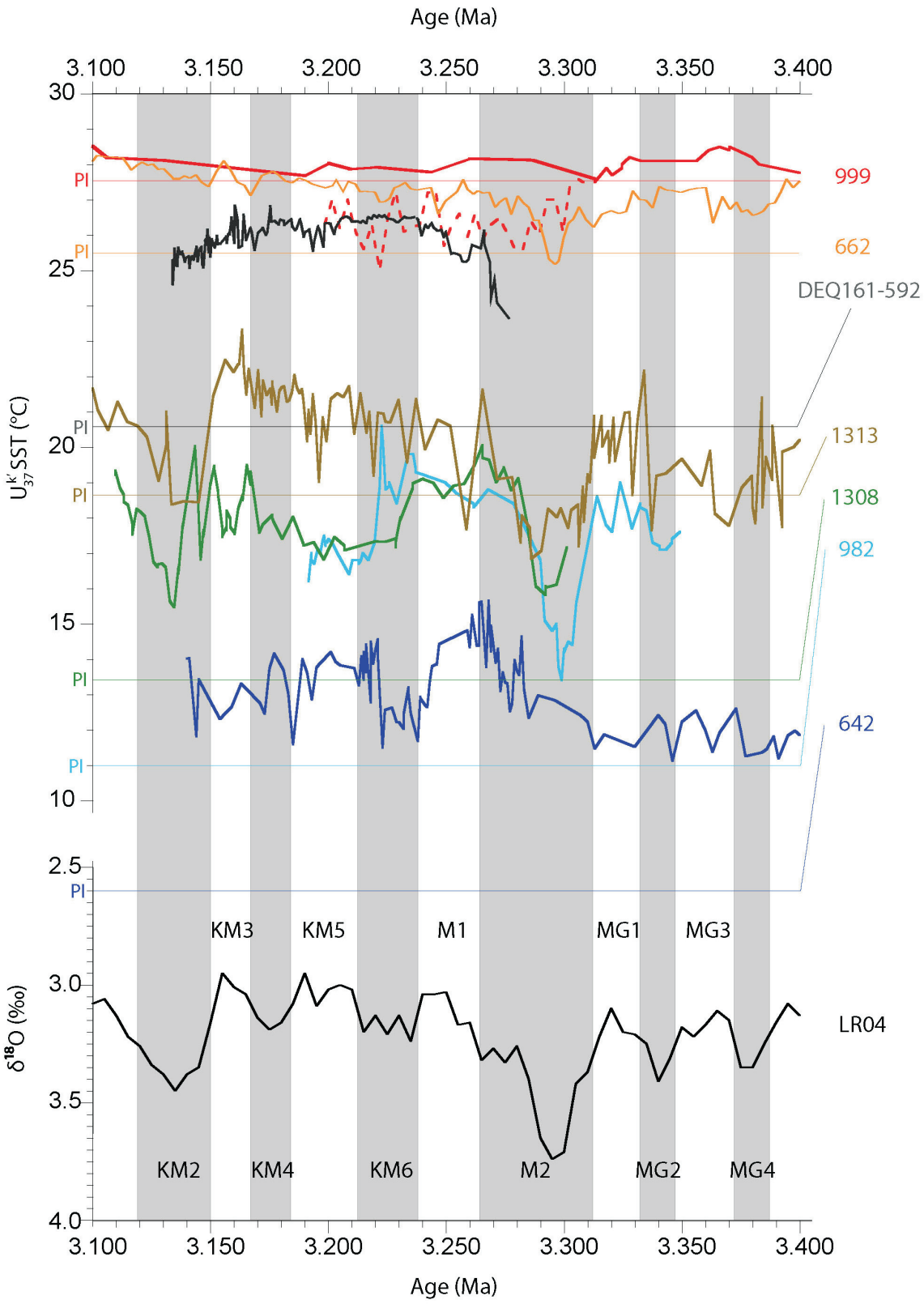

TEXT-FIGURE 5
Comparison of North Atlantic alkenone sea surface temperature (SST) time series data and LR04 benthic oxygen isotope stack (Lisiecki and Raymo 2005) between 3.4 Ma and 3.1 Ma. Glacial stages shaded gray. Dashed red line shows Site 999 estimates based upon a faunal transfer function. Solid red line alkenone based estimates from Badger et al. (2013) and Dowsett et al. (2017). Alkenone SST estimates for Site 642 (Bachem et al. 2016); Site 1313 (Naafs et al. 2012; Dowsett et al. 2017); Site 662 (Herbert et al. 2010); Sites 982, 1308 and DEQ161-592 (Dowsett et al. 2017). Thin horizontal lines indicate pre-industrial (PI) SST for each site (Huang et al. 2017).

sional gaps created by bottom currents, both of which can remain undetected in cored sequences. Due to the nature of marine sediments, a truly synchronous reconstruction is unrealizable.

High-resolution benthic oxygen isotope sequences improve the accuracy of locating a defined mid-Piacenzian interval in individual records and provide the key to correlating this interval between localities. Correlation across an ocean basin, however, is still complicated by leads and lags in the global ice volume signal and by regional climate dynamics, both of which are encapsulated in the benthic oxygen isotope record. Even the correct alignment of $\delta^{18}O$ records contains some uncertainty. Lisiecki and Raymo (2005) caution that aligning benthic $\delta^{18}O$ records from different oceanographic settings could produce age model errors of several thousand years. We incorporate alkenone records in an attempt to reduce uncertainties in chronology and correlation, and to sharpen stratigraphic resolution in coastal plain sequences. Our alkenone estimates of SST provide high signal-to-noise ratios for robust correlation, but this surface-influenced proxy signal may not be synchronous over long distances.

The Pliocene itself offers a challenge to chronostratigraphic correlations; the amplitude of typical glacial-interglacial cycles is reduced by about 40% relative to the late Pleistocene (e.g., Lisiecki and Raymo, 2005). The increased dominance of obliquity cycles in the Pliocene, relative to the late Pleistocene, also results in fewer distinctive features for correlation, increasing the risk of misidentifying isotopic stages and miscorrelating paleoclimatic information. Because the greatest orbital-scale variance during the mid-Piacenzian is in the obliquity band (41 ky cycles), at a minimum, sample resolution must be able to distinguish between obliquity cycles in order to correlate records. To capture the several short-lived, intense glacial-interglacial features that appear in mid-Piacenzian isotopic records (e.g., MIS M2 and KM5c), sample spacing needs to be equal to or better than 5 ky.

Synoptic climate reconstructions of specific time intervals during the mid-Piacenzian incorporate inherent uncertainties related to the identification of the correct chronostratigraphic interval in each record, the correlation of this interval precisely across records, and the synchroneity of tie points. Even with careful work to minimize uncertainties in our chronostratigraphic correlations, some remain. While it is unclear if the irregular alignment of MIS M2 among sites in text-figure 5 is due to misinterpretation of the records or to the potentially diachronous nature of the event, where we have $\delta^{18}O$ in conjunction with alkenones, the synchrony is clear. We expect further stratigraphic work will improve the correlation.

Sea-Surface Temperature Gradient

A wealth of marine fossil data suggests a North Atlantic warm anomaly in the Pliocene, increasing in magnitude from the Caribbean toward the Arctic (e.g., Dowsett et al. 1992; Cronin et al. 1993; Bartoli et al. 2005; Groeneveld 2005; Robinson et al. 2008; Sarnthein et al. 2009; Lawrence et al. 2009; Herbert et al. 2010; De Shepper et al. 2013). Circum-Atlantic pollen and plant macrofossils are in general agreement (e.g., Willard 1994, 1996; Ballantyne et al. 2010; Salzmann et al. 2008, 2013; Panitz et al. 2018). Dowsett et al. (1992) showed that the Pliocene North Atlantic SST gradient exhibited amplification toward polar regions unlike that expected from warming due solely to increased radiative trace gasses (Rind and Chandler 1991). The PRISM3 SST reconstruction further documented polar amplification in other ocean basins based upon multiple proxies, which has proven difficult for climate models to simulate (Dowsett et al. 2012, 2013a).

Some data previously used to construct the Pliocene North Atlantic gradient no longer fall within age limits of the PRISM interval. For example, analysis of dinoflagellates at Tjornes, Iceland, revised the age of the base of the Serripes Zone, which marks an opening of the Bering Strait and invasion of Pacific mollusks to the Atlantic via the Arctic. These beds are now dated to the Zanclean (Verhoeven et al. 2011) and thus should not be considered in the construction of a Piacenzian North Atlantic surface temperature gradient. In addition, previous use of multiple proxies to establish the North Atlantic SST gradient was somewhat flawed. Agreement between different temperature proxies was thought to establish more robust estimates. With recognition that temperature proxies (i.e. Mg/Ca, TEX86, Faunal, $U^{k'}_{37}$) measure different aspects of temperature, it makes little sense to look for agreement between them. Instead, differences in temperature proxies are more appropriately used to form a more complete understanding of the paleoenvironmental setting, in time and space (Dowsett et al. 2013b).

We have chosen to use a pre-industrial mean annual sea surface temperature (PI SST) field as a base from which to derive PRISM4 Pliocene temperature anomalies (Table 1; Supplement). We use the 1870-1899 average from the NOAA Extended Reconstructed SST.v5 (Huang et al. 2017). PI SST conditions are shown in Table 1, along with PRISM4 SST estimates and anomalies (Pliocene mean annual SST minus PI SST). Note that while we use the same Site 642 alkenone SST data provided by Bachem et al. (2016), we correct anomalies shown in that work to reflect the difference from PI conditions, rather than a Holocene average, thus making comparison to climate models possible.

Given the refinement in chronologic resolution and the move from multiple proxies to a single paleothermometer, we might expect the PRISM4 North Atlantic surface temperature gradient to be different than was initially proposed for the mid-Pliocene. Instead, the new gradient, derived solely from $U^{k'}_{37}$ SST estimates associated with MIS KM5c (Table 1), is nearly indistinguishable from the original (text-fig. 8). This suggests the shape of the North Atlantic surface temperature gradient is a robust feature of the Pliocene climate, and changes in proxy and uncertainty in age have little effect on the slope. Still, until recently, models have been unable to simulate the amount of warming indicated for higher latitudes. Adjustments in the bathymetry of major ocean gateways in climate models has led to model simulations that more closely resemble the PRISM4 temperature gradient (Otto-Bliesner et al. 2017). Feng et al. (2017) also showed amplified late Pliocene terrestrial warmth in high northern latitudes in simulations using a *closed* Bering Strait and Canadian Arctic Archipelago. The pattern of warmth agrees with but still underestimates that suggested by terrestrial temperature proxies (Elias and Matthews 2002; Ballantyne et al. 2010, 2013; Brigham-Grette et al. 2013; Salzmann et al. 2008, 2013).

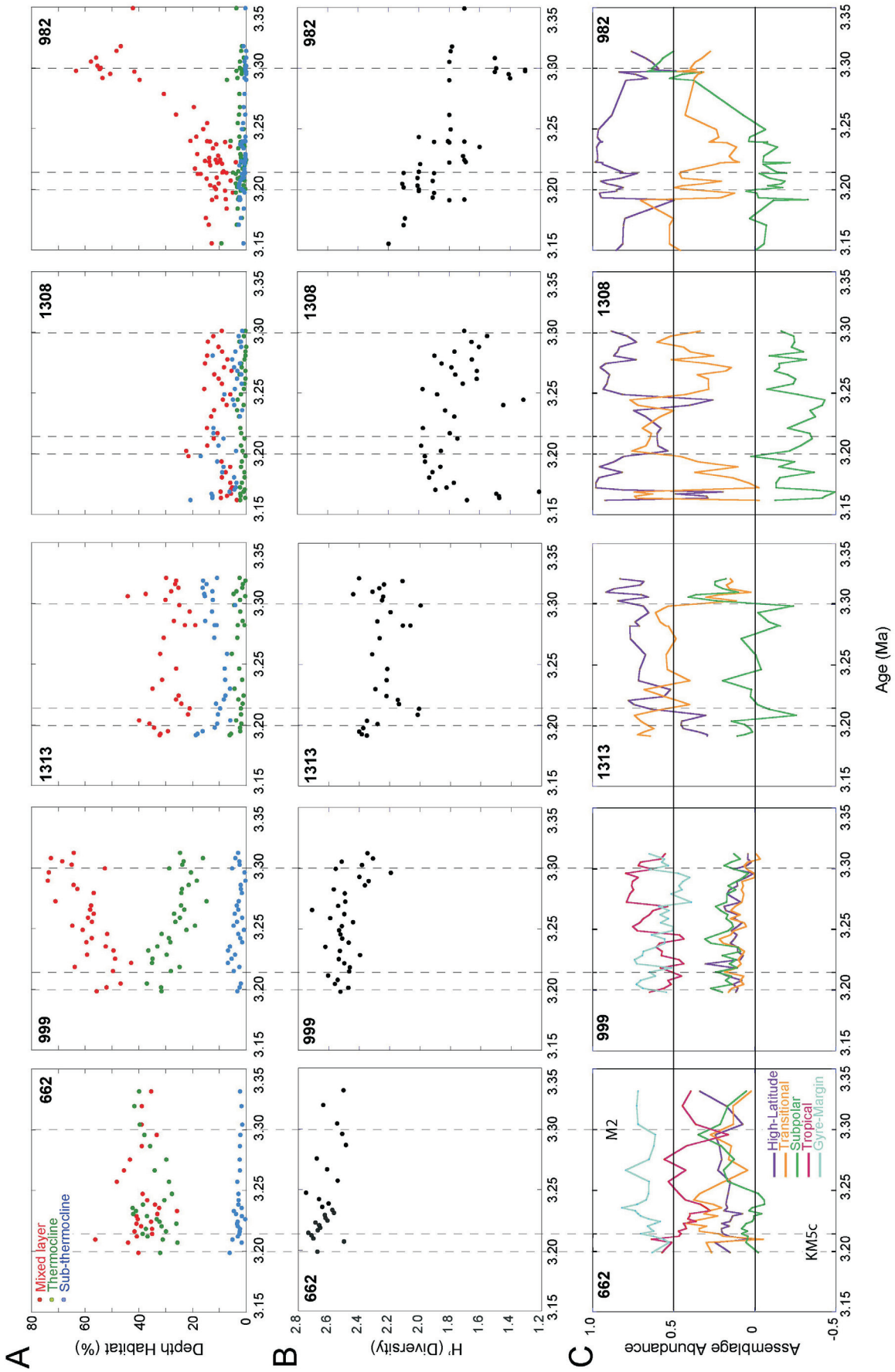

TEXT-FIGURE 6
A. Abundance of mixed layer (red), thermocline (green) and sub-thermocline (blue) foram ecogroups of Aze et al. (2011). B. Shannon Diversity (H') values. C. Abundance of mid-Piacenzian planktonic foraminifer assemblages in the North Atlantic at each site. Vertical dashed lines are guides to 3.20 Ma, 3.21 Ma (MIS KM5c) and 3.3 Ma (peak MIS M2).

Role of Ocean Gateways

Central American Seaway

The closing of the Central American Seaway (CAS) has been used to explain many observed paleoceanographic patterns in the Caribbean Sea and North Atlantic Ocean including sea surface warming (e.g., Berggren and Hollister 1974; Keigwin 1982; Coates et al. 1992; Cronin and Dowsett 1996, Haug and Tiedemann 1998; Haug et al. 2001; Steph et al. 2006, Sarnthein et al. 2009; De Schepper et al. 2013; Karas et al. 2017). CAS closure was gradual, with final closure occurring over at least two million years, interrupted by multiple re-openings (O'Dea et al. 2016).

Micropaleontological data from the shallow marine record of Central America, the Atlantic Coastal Plain of North America, and Caribbean deep-sea core sites (e.g., Hazel 1971; Cronin and Dowsett 1990; Cronin 1991; Dowsett et al. 1992; Haug and Tiedemann 1998) suggest that prior to 4 Ma the CAS was open, and cooler and less saline than the marine waters that characterize the shelf off eastern North America today. Benthic faunas do not show evidence of warm Gulf Stream waters moving north (Johnson et al. 2017), and planktonic assemblages suggest low salinity in the Caribbean at this time (Cronin and Dowsett 1996). Shoaling of the CAS to less than 100 m depth by 4 Ma may have led to increased warmth (and increased salinity) in the North Atlantic, which in turn could have increased thermohaline circulation (Karas et al. 2017).

By ~3.3 to 3.0 Ma, warming, relative to PI conditions, occurred along the east coast of North America and in the mid to high latitudes of the North Atlantic (Dowsett 2007; Sarnthein et al. 2009; Dowsett et al. 2009; 2010). In the Caribbean, planktonic foraminifer diversity and abundance of upwelling indicators increase following MIS M2 through KM5, and higher frequency variations coincide with changes in abundance of *Gs. sacculifer* and *Dentoglobigerina altispira.* Both taxa have maximum abundances at the base of the investigated Site 999 sequence (text-fig. 4). We attribute repeated decline followed by recovery of these taxa in the Caribbean to cyclical freshening due to intermittent inflow of lower salinity Pacific water throughout the late Pliocene. This is also seen in the Site 999 assemblage data as an alternation in the relative strength of the tropical assemblage (warmer conditions, closed CAS) and gyre margin assemblage (cooler lower salinity, open CAS). During the ~3.3 to 3.0 Ma interval we see a continuous decrease in the abundance of mixed layer taxa suggesting an overall shallowing of MLD.

Farther north on the Atlantic Coastal Plain, repeated transgressive pulses followed by regressions and associated unconformity surfaces (see Ward and Blackwelder 1980) can be correlated to offshore records and dated using the LR04 timescale. The MIS M2 event on the Atlantic Coastal Plain of Virginia is recognized by a major unconformity at the base of the Rushmere Member of the Yorktown Formation. Sediments below this unconformity are either Zanclean (Sunken Meadows Member of the Yorktown Formation) or Messinian (belonging to the Miocene Eastover Formation), depending upon location. The Rushmere is interpreted to be a rapidly transgressive unit deposited during the M2/M1 transition. The conformably overlying Morgarts Beach Member then represents sediment accumulation during the M1 – KM5 interglacials. These rhythmic sedimentary packages further document changes in sea level and Gulf Stream warmth during the period of closure of the CAS.

Bering Strait

Paleontological evidence suggests Pacific water flowed through the Bering Strait into the Arctic and then into the North Atlantic during the Zanclean (Gladenkov et al. 1991; Marincovich and Gladenkov 1999, 2001; Verhoeven et al. 2011). Faunal exchange of thermophilic ostracodes between the Atlantic and Pacific via the Arctic also supports an open Bering Strait and warmer Arctic conditions during at least parts of the Pliocene and early Pleistocene (Cronin et al. 1993; Matthiessen et al. 2009). This has previously been the justification for an open Bering Strait in mid-Piacenzian paleogeographic reconstructions and climate model experiments. Contrarily, there is *no* evidence to suggest that the strait remained continuously open. Given the tectonic activity in the region, the current shallow (~50 m) depth of the strait, and magnitude of glacioeustatic sea level changes, it seems likely the Bering Strait would have undergone multiple closures during the Pliocene, similar to the CAS.

Unlike previous PRISM reconstructions, our PRISM4 paleogeography considers first order effects of mantle convection (Rowley et al. 2013) in addition to glacial isostatic adjustments and retrodicts a closed Bering Strait for the mid-Piacenzian (Dowsett et al. 2016). Closing of the Bering Strait has the effect of reducing transport of relatively fresh water from the Pacific to the Arctic and North Atlantic, increasing salinity in the high latitude North Atlantic, thereby strengthening the Atlantic Meridional Overturning Circulation (AMOC), and increasing meridional ocean heat transport (Hu et al. 2015; Feng et al. 2017; Otto-Bliesner et al. 2017).

PlioMIP simulations using a closed CAS and open Bering Strait show a range of climate responses that suggest a reduced or similar (to control) AMOC and a smaller mid-to-high latitude SST anomaly than estimated from proxy data for the mid-Piacenzian (Haywood et al. 2013b, Zhang et al. 2013). However, Feng et al. (2017) and Otto-Bliesner et al. (2017) show an increased high latitude temperature anomaly relative to the PlioMIP experiment, resulting from closing northern hemisphere ocean gateways. PlioMIP2 experimental protocols use the PRISM4 paleogeography featuring a closed CAS, closed Bering Strait and closed Canadian Archipelago (Dowsett et al. 2016). This cuts off inflow of Pacific waters to the Arctic and effectively restricts communication between the Arctic and North Atlantic through the Fram Strait. Initial PlioMIP2 results using these boundary conditions (e.g., Kamae et al. 2016; Chandan and Peltier 2017, 2018; Zheng et al. 2018; Hunter et al. 2019) show an enhanced high-latitude SST anomaly, consistent with proxy reconstructions, which can be attributed directly or indirectly to the closed state of the Bering Strait in the PRISM4 reconstruction.

Greenland – Scotland Ridge

Carbon isotope records show that North Atlantic Deep Water overflowing the Greenland – Scotland Ridge (GSR) during the mPWP was strong, relative to present day, and decreased following the Late Pliocene (Oppo and Fairbanks 1987; Wright and Miller 1996; Poore et al. 2006). The PRISM4 paleogeographic reconstruction shows a deeper than pre industrial GSR during the Piacenzian. Robinson et al. (2011) showed changes

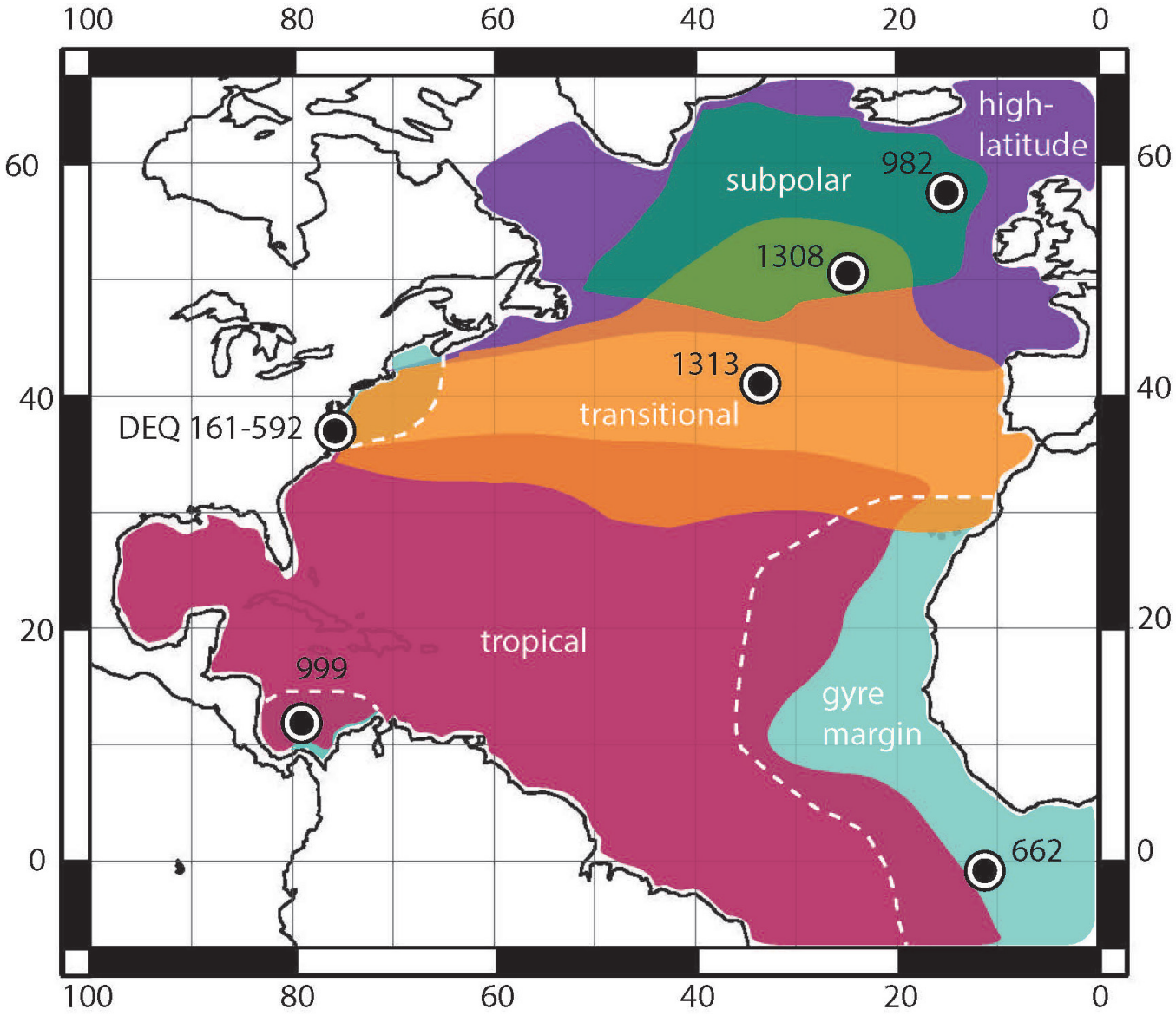

TEXT-FIGURE 7
Distribution of North Atlantic planktonic foraminifer assemblages recovered from core-top sediment samples. Colors show regions of maximum importance of end-member high latitude, sub-polar, transitional, tropical and gyre margin assemblages. White dashed lines highlight boundary of gyre margin assemblages. Bullets show core site locations where Pliocene faunal data were developed.

related to a deeper GSR could have increased heat transport from the North Atlantic to the Arctic Ocean.

Data Model Comparison

Documenting the evolution of paleoenvironmental conditions at a number of sites through evaluation of time-series data provides invaluable insight to the overall dynamics of the Pliocene climate system. However, paleoclimate model experiments generally produce temporal "snapshots" of conditions making synoptic reconstructions more useful for data-model comparison. Previous PlioMIP comparisons used paleoenvironmental estimates that represented a time-averaged equilibrium climate to verify simulated conditions (Dowsett et al. 2012, 2013a; Salzmann et al. 2013). In an effort to reduce uncertainty, PlioMIP2 experimental protocols require comparison data at orbital scale resolution targeted at a stratigraphic horizon that exhibits orbital forcing close to that of present day. The chosen interval was within the mid-Piacenzian (text-fig. 1), centered at 3.205 Ma, and corresponds to MIS KM5c (Haywood et al. 2013a, 2016b).

We have limited our North Atlantic reconstruction to those sites where alignment to MIS KM5c of the LR04 stack was achievable and we are depending upon accurate age models. This necessitates that both the tuning of each site to the LR04 stack, and calibration of LR04 to absolute time are correct. We compare PRISM4 North Atlantic $U^{k'}_{37}$ SST anomalies from Sites 662, 999, DEQ161-592, 1313, 1308, 982 and 642 to a

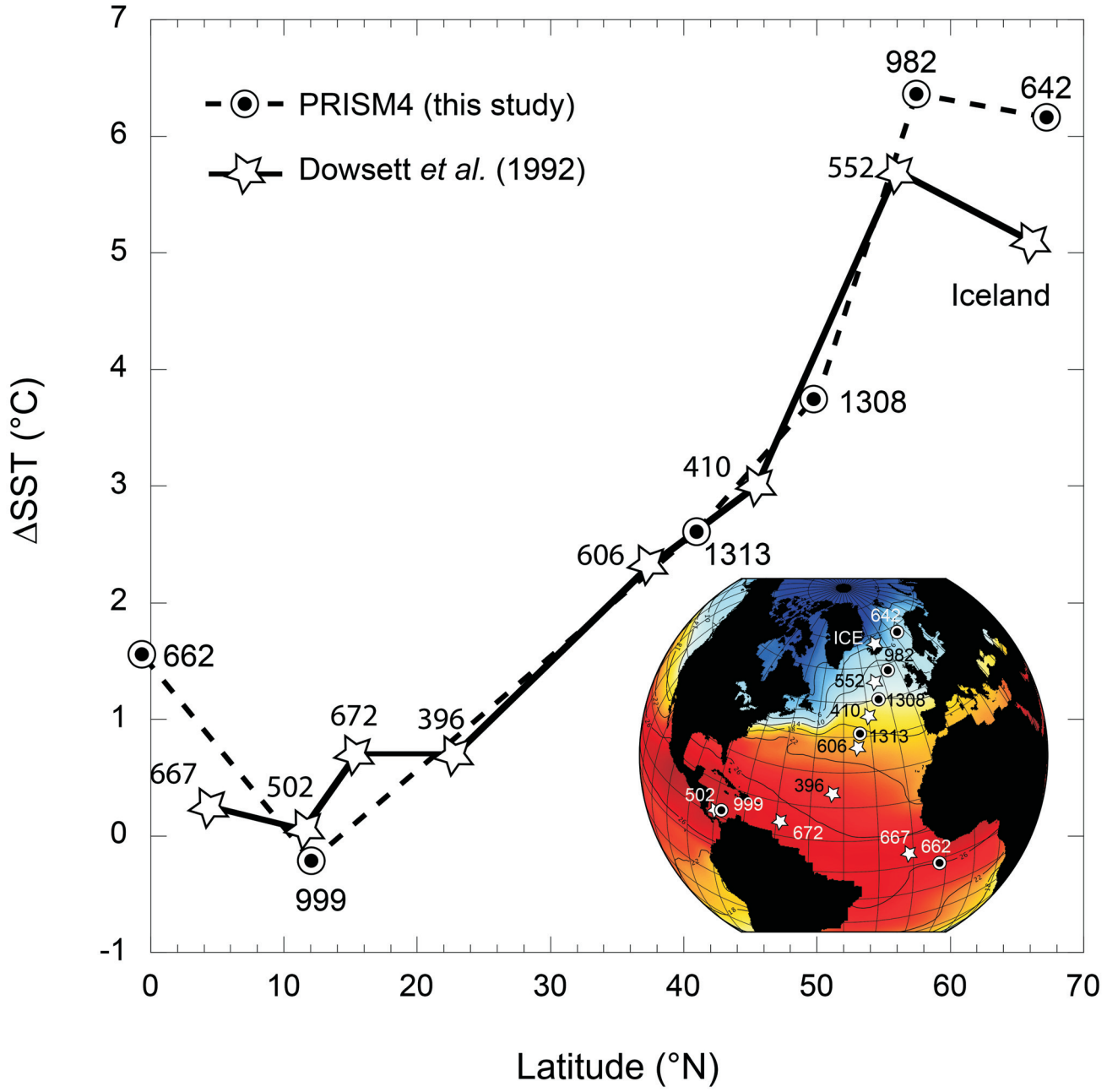

TEXT-FIGURE 8
Comparison of North Atlantic Pliocene mean annual sea surface temperature (SST) anomaly profiles (mid-Piacenzian – pre-industrial) after Dowsett et al. (1992; stars) and PRISM4 estimates from this study (bullets). Location of sites shown in the inset map are projected on NOAA pre-industrial (1870-1899 AD) mean annual SST (Huang et al. 2017). Scale same as in Text-figure 2.

model experiment by Otto-Bliesner et al. (2017) using the Community Climate System Model Version 4 (CCSM4). While the boundary conditions are not precisely the same as in PRISM4 (Dowsett et al. 2016), the simulations do show the relative effects of a closed Bering Strait and closed Canadian Arctic Archipelago. We compare the experiments with paleogeographic changes to PlioMIP1 results that used the same model (Rosenbloom et al. 2013) as well as our new PRISM4 SST data (text-fig. 9).

In the tropics and at the mid latitude coastal plain site, all three simulations are basically the same in that they show changes in northern ocean gateways have little effect. The agreement between the simulations and our alkenone SST estimates are close in the tropics (text-fig. 9). At our Atlantic Coastal Plain site, the differences between PRISM4 and CCSM4 anomalies are greater than 4°C. This result is not surprising as the DEQ 161-592 site is presently located on land and therefore it's not possible to compare model and

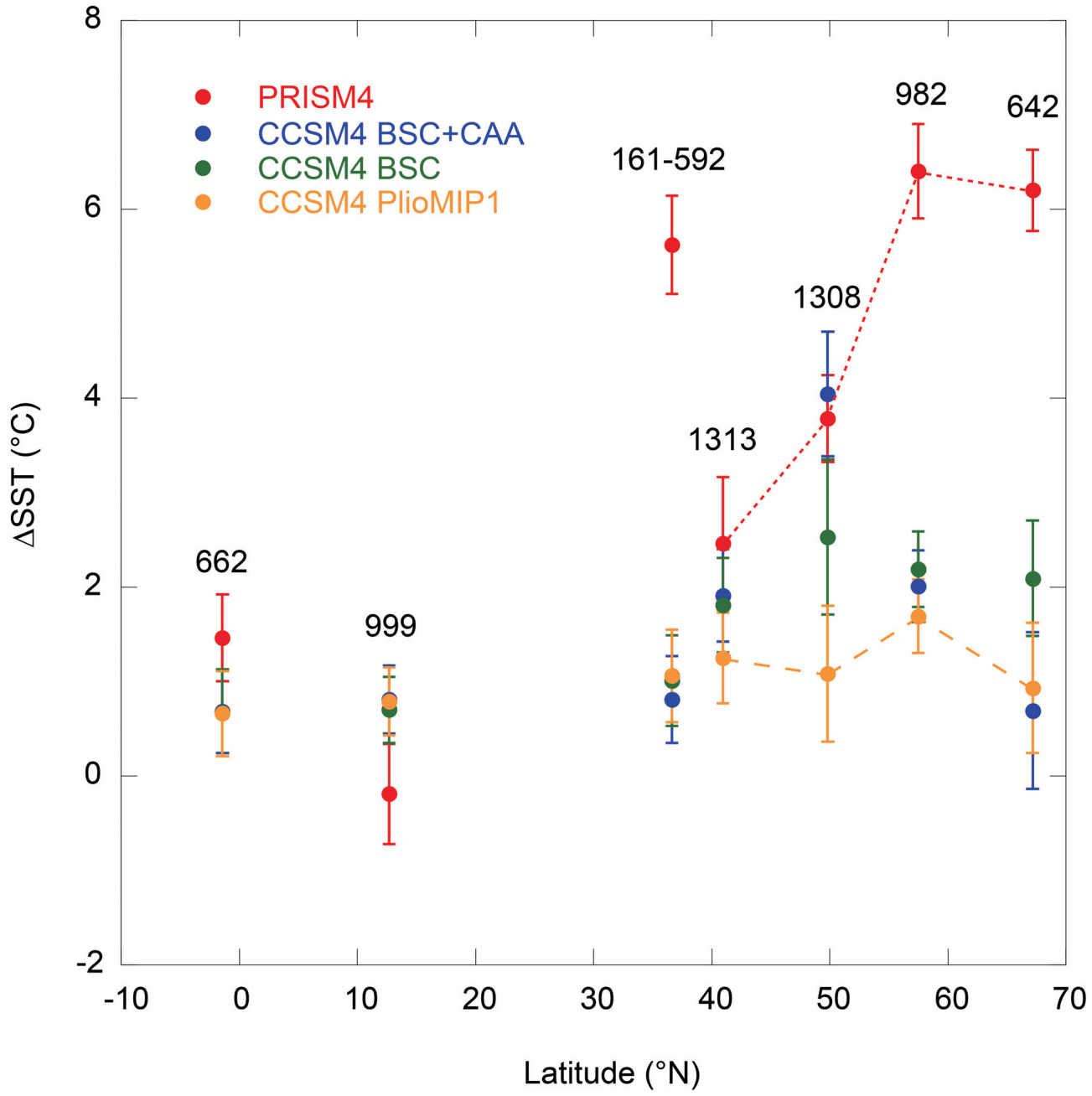

TEXT-FIGURE 9
Comparison of SST anomalies within the PlioMIP2 timeslice from PRISM4 (red) and NCAR CCSM4 simulations using PlioMIP1 boundary conditions (orange) and the same with a closed Bering Strait (green) and closed Bering Strait and closed Canadian Arctic Archipelago (blue) from Otto-Bliesner et al. (2017). Combined uncertainty bars for alkenone anomalies are estimated as the square root of the sum of the squares of σSST_{pi} and $\sigma SST_{plio.}$ Combined uncertainty for model anomalies are calculated the same way using σSST_{model} and σSST_{ctrl}. See also Table 1.

data SST's from the same location. For comparison with the models, especially those that use a modern land mask, we chose the spatially closest ocean grid cell in CCSM4. Today, the Gulf Stream diverges from North America at Cape Hatteras. The Carolina Coastal Current is a weaker northward flowing warm current, south of Cape Hatteras. The Virginia Coastal Current flows south bringing cool water toward Cape Hatteras. The potential shift in the gyre to a more northerly position and the variability of the Carolina and Virginia Coastal Currents, combined with a simulation using modern paleogeography, makes comparison problematic. Thus, while the site is useful for understanding paleoenvironmental conditions in the North Atlantic, it is not particularly useful for locality-based data-model comparison. We anticipate similar issues with elements of the PlioMIP2 ensemble that choose to use a modern (present-day) coastline.

At Sites 1313, 1308, 982 and 642, the inclusion of a closed Bering Strait increases CCSM4 SST anomalies relative to the PlioMIP1 result, moving the model simulations closer to the alkenone-based SST anomalies. At Sites 1313 and 1308, considering the uncertainty of both estimated and simulated temperatures, the model and data are now in agreement. Although inclusion of the closed Canadian Arctic Archipelago decreased the model-data discord at Site 982, it resulted in a smaller anomaly than with just the Bering Strait closed. In the Norwegian Sea (Site 642) adding the closed Canadian Arctic Archipelago to the closed Bering Strait scenario reduces the SST anomaly to the PlioMIP1 level. Interestingly, an unpublished CCSM4 simulation with closed gateways and improved vegetation boundary conditions warms sites 982 and 642 an additional ~2°C as compared to just the closed gateway simulations (R. Feng personal communication). A comparison of the PRISM4 North Atlantic with all PlioMIP2 models should provide additional insight on the effect of the PRISM4 boundary conditions.

With the myriad issues associated with chronologic uncertainty, and the sensitivity of models to the position of important currents or oceanographic fronts, it may be that rather than a site by site comparison with limited amounts of proxy data, robust patterns and overall magnitudes of large-scale features would be a more useful measure of agreement between models and data. Feng et al. (2017) used a pattern recognition technique to simplify the surface temperature field produced by the model to a small number of representative patterns that could be more easily compared to the limited amount of terrestrial paleoenvironmental data. A similar approach could be used with the relatively sparse (when compared to model output which has a value for every grid box) SST data. Thus, while we used a point-by-point comparison between a small number of sites and the CCSM4 SST of Otto-Bliesner et al. (2017), we suggest reproducing the slope and magnitude of the pole to equator surface temperature gradient, or perhaps the temperature difference between the tropics and mid latitudes, may be a better way to compare models to models and models to data. Such an approach avoids the tendency to reduce data-model comparison to a comparison of compounded uncertainties. Comparing model output other than surface temperature (e.g. mixed layer depth, salinity, productivity, nutrients) to faunal and alkenone data that measure similar variables may also result in a more informative comparison. For example, two models may match SST estimates provided by the proxy community, but the model that also agrees with MLD changes and relative position of fronts or other features reconstructed through biomarkers and biogeographic analysis of faunal data, would provide a more robust result. A global comparison of an ensemble of PlioMIP2 simulations to PRISM4 data, and a community sourced verification data set (see Foley and Dowsett 2019) for the mid-Piacenzian, is in preparation.

SUMMARY AND CONCLUSIONS

Research into deep-time climates (e.g. the Pliocene, Eocene and Cretaceous) has led to profound increases in our understanding of the climate system, which in turn are directly relevant to a better understanding of future change. Rather than use methodologies best applied to historical and Holocene materials (possessing near-continuous time control) on deep-time archives, it seems apparent that instead we should attempt to identify robust environmental patterns and rephrase questions that deep-time geoarchives are uniquely positioned to answer. This will potentially lead to more nuanced interpretations of changing paleoenvironments in the face of sweeping climate changes and a more realistic assessment of model performance.

MIS M2/M1

Conditions at MIS M2 were consistently colder than PI across the North Atlantic Basin. These cool conditions were associated with increased seasonality and a sea level drop documented by a widespread unconformity on the Atlantic Coastal Plain. The initial part of the M2/M1 transition shows increasing faunal diversity as well as increasing SST at all sites.

MIS KM5c

The Central American Isthmus was in place and the Central American Seaway closed at this time. We confirm a small ~1.5 °C SST anomaly (Pliocene minus PI) at the equator. Warmer than PI conditions can be documented along the coast of North America and on across the Atlantic following the North Atlantic Drift where the northern limb of the subtropical gyre was shifted north relative to present day. This warmer than PI condition extended to at least 67° North in the Norwegian Sea. Open ocean sites show a Pliocene surface temperature anomaly increasing with latitude from ~1.5°C near the equator to >6°C near 60° North.

Deep-time data model comparison

There are limits to the temporal and spatial resolution obtainable from deep-time geoarchives. Non-linear and discontinuous sediment accumulation coupled with intermittent and highly variable sediment mixing due to bioturbation and other physical processes, in all but a few unique environments, is problematic. Any increase in the acuity to which we understand and can reconstruct the environment, temporally, spatially, or dynamically, is met with a decrease in confidence of that understanding, due to increasing numbers of assumptions. The confidence, in qualitative terms, of knowing the 3.205 Ma level in any one core, let alone correlating that level at multiple sites, is not high. However, orbital conditions do not show much change in forcing over almost 20,000 years on either side of KM5c, thus age control for PlioMIP2 experiments can be somewhat relaxed (Prescott et al. 2014).

The paleogeographic component of the PRISM4 reconstruction, with a closed Bering Strait and closed Central American Seaway, results in a better fit of models and proxy temperature data. These results would suggest an increase in AMOC and North Atlantic Deep Water (NADW) formation during at least parts of the Piacenzian. If PlioMIP2 simulations do show an increased strength of AMOC, it must be reconciled with several lines of evidence that call for a more sluggish circulation at this time.

Reinterpretation of fauna

Habitat suitability is controlled by a number of factors and multiple examples of faunal abundance patterns tracking environmental changes other than temperature present an opportunity, and argue for increased efforts, to understand complex multifactor paleoecological relationships. These, in turn, may lead to better and more realistic tests of our confidence in Earth System Models than conventional comparisons of SST.

Data Availability\

Faunal data generated as part of this study can be found at https://www.ncdc.noaa.gov/paleo/study/27310.

Author contributions

HJD conceived and designed the study. HJD, MMR, KMF, TDH and BO-B contributed and analyzed data. All authors prepared the manuscript.

Competing interests

The authors declare no conflict of interest.

ACKNOWLEDGMENTS

HJD acknowledges support from the U.S. Geological Survey Land Change Science Program. TDH acknowledges support from NSF grant OCE-1459280. BO-B acknowledges the National Center for Atmospheric Research (NCAR), which is a major facility sponsored by the NSF under Cooperative Agreement No. 1852977. The CESM project is supported primarily by the National Science Foundation (NSF). Computing and data storage resources, including the Cheyenne supercomputer (doi:10.5065/D6RX99HX), were provided by the Computational and Information Systems Laboratory (CISL) at NCAR. We thank the Virginia Department of Environmental Quality (DEQ) for information and access to core DEQ161-159. This research used samples and/or data provided by the Ocean Drilling Program (ODP) and International Ocean Discovery Program (IODP). This is a product of the PRISM4 (Paleoclimate Data Model Synergy) and GIN (Geological Investigations of the Neogene) Projects. Diversity estimates were computed using EstimateS (Version 9). Any use of trade, firm, or product names is for descriptive purposes only and does not imply endorsement by the U.S. Government.

REFERENCES

AHN, S., KHIDER, D., LISIECKI, L. E. and LAWRENCE, C. E., 2017. A probabilistic Pliocene–Pleistocene stack of benthic $\delta^{18}O$ using a profile hidden Markov model. *Dynamics and Statistics of the Climate System,* 2:1–16, https://doi.org/10.1093/climsys/dzx002

AZE, T., EZARD, T. H., PURVIS, A., COXALL, H. K., STEWART, D. R., WADE, B. S. and PEARSON, P. N., 2011. A phylogeny of Cenozoic macroperforate planktonic foraminifera from fossil data. *Biological Reviews*, 86: 900–927, doi:10.1111/j.1469-185X.2011.00178.x

BACHEM, P. E., RISEBROBAKKEN, B. and MCCLYMONT, E. L., 2016. Sea surface temperature variability in the Norwegian Sea during the late Pliocene linked to subpolar gyre strength and radiative forcing. *Earth and Planetary Science Letters,* 446:113–122.

BADGER, M. P. S., SCHMIDT, D. N., MACKENSEN, A. and PANCOST, R. D., 2013. High resolution alkenone palaeobarometry indicates relatively stable pCO2 during the Pliocene (3.3 to 2.8 Ma). *Philosophical Transactions of the Royal Society A,* 373: 20130094.

BALLANTYNE, A.P., AXFORD, Y., MILLER, G.H., OTTO-BLIESNER, B.L., ROSENBLOOM, N. and WHITE, J.W., 2013. The amplification of Arctic terrestrial surface temperatures by reduced sea-ice extent during the Pliocene. *Palaeogeography, Palaeoclimatology, Palaeoecology*, 386: 59–67.

BALLANTYNE, A., GREENWOOD, D., DAMSTÉ, J. S., CSANK, A., EBERLE, J. and RYBCZYNSKI, N., 2010. Significantly warmer Arctic surface temperatures during the Pliocene indicated by multiple independent proxies. *Geology*, 38: 603–606.

BARTOLI, G., SARNTHEIN, M., WEINELT, M., ERLENKEUSER, H., GARBE-SCHONBERG, D. and LEA, D.W., 2005. Final closure of Panama and the onset of northern hemisphere glaciation. *Earth and Planetary Science Letters*, 237: 33–44.

BÉ, A. W. H., 1977. An ecological, zoogeographic and taxonomic review of recent planktonic foraminifera. In: Ramsay, A. T. S., Ed., *Oceanic Micropaleontology,* 1–100. London: Academic Press.

BERGGREN, W. A. 1973. The Pliocene Time Scale: Calibration of Planktonic Foraminiferal and Calcareous Nannoplankton Zones. *Nature,* 243: 391–397.

BERGGREN, W. A. and HOLLISTER, C. D., 1974. Paleogeography, paleobiogeography, and the history of circulation in the Atlantic Ocean. In: Hay, W.W., Ed., *Studies in Paleoceanography*, Special Publication, 126–186. Tulsa: Society of Economic Paleontologists.

BLOW, W. H., 1969. Late middle Eocene to recent planktonic foraminiferal biostratigraphy. In: Bronniman, P. and Renz, H.H., Eds., *Proceedings of the 1st International Conference on Planktonic Microfossils*, 199–422. Leiden: E.J. Brill.

BOLTON, C. T., LAWRENCE, K. T., GIBBS, S. J., WILSON, P. A., CLEAVELAND, L. C. and HERBERT, T. D., 2010. Glacial-interglacial productivity changes recorded by alkenones and microfossils in late Pliocene eastern equatorial Pacific and Atlantic upwelling zones, *Earth and Planetary Science Letters*, 295: 401–411, 10.1016/j.epsl.2010.04.014.

BRIGHAM-GRETTE, J., MELLES, M., MINYUK, P., ANDREEV, A., TARASOV, P., DECONTO, R., KOENIG, S., NOWACZYK, N., WENNRICH, V., ROSÉN, P., HALTIA, E., COOK, T., GEBHARDT, C., MEYER-JACOB, C., SNYDER, J. and HERZSCHUH, U., 2013. Pliocene Warmth, Polar Amplification, and Stepped Pleistocene Cooling Recorded in NE Arctic Russia. *Science*, 340: 1421–1427.

CHANDAN, D., and PELTIER, W. R., 2017. Regional and global climate for the mid-Pliocene using the University of Toronto version of CCSM4 and PlioMIP2 boundary conditions. *Climate of the Past*, 13: 919–942, 10.5194/cp-13-919-2017.

_____, 2018. On the mechanisms of warming the mid-Pliocene and the inference of a hierarchy of climate sensitivities with relevance to the understanding of climate futures. *Climate of the Past*, 14: 825–856. 10.5194/cp-14-825-2018.

CHEN, M.-T. 1994. Estimating thermocline from planktonic foraminifer faunal data: the development of paleoecological transfer functions for reconstructing low-latitude Pacific upper-layer conditions. *Journal of the Geological Society of China,* 37: 443–474.

COATES, A., JACKSON, J. B. C., COLLINS, L. S., CRONIN, T. M., DOWSETT, H. J., BYBELL, L. M., JUNG, P. and OBANDO, J. A., 1992. Closure of the Isthmus of Panama: The near-shore marine record of Costa Rica and western Panama. *Geological Society of America Bulletin*, 104: 814–828, 10.1130/00167606(1992)104<0814:cotiop>2.3.co;2

COLWELL, R. K., 2013. EstimateS: Statistical estimation of species richness and shared species from samples, Version 9. User's Guide and application published at:http://purl.oclc.org/estimates.

CRONIN, T. M., 1991. Pliocene shallow water paleoceanography of the North Atlantic Ocean based on marine ostracodes. *Quaternary Science Reviews*, 10: 175–188, 10.1016/0277-3791(91)90017-O

CRONIN, T. M., and DOWSETT, H. J., 1990. A quantitative micropaleontologic method for shallow marine paleoclimatology: Application to Pliocene deposits of the western North Atlantic Ocean. *Marine Micropaleontology*, 16:117–147, 10.1016/0377-8398(90)90032-H

———, 1996. Biotic and oceanographic response to the Pliocene closing of the Central American isthmus. In: Jackson, J. B. C., Budd, A. F.,

and Coates, A. G., Eds., *Evolution and environment in tropical America,* 76–104. Chicago: University of Chicago Press.

CRONIN, T. M., DOWSETT, H. J., GOSNELL, L. B. and ROSS, R. M. 1989. Pliocene marine micropaleontology of southeastern Virginia and northeastern North Carolina *U.S. Geological Survey, Open-File Report* 89-678:16pp.

CRONIN, T. M., WHATLEY, R., WOOD, A., TSUKAGOSHI, A., IKEYA, N., BROUWERS, E. M. and BRIGGS, W. M., Jr., 1993. Microfaunal Evidence for Elevated Pliocene Temperatures in the Arctic Ocean. *Paleoceanography*, 8: 161–173, 10.1029/93PA00060

DE SCHEPPER, S., HEAD, M. J. and GROENEVELD, J., 2009. North Atlantic Current variability through marine isotope stage M2 (circa 3.3 Ma) during the mid-Pliocene. *Paleoceanography*, 24:PA4206, 10.1029/2008pa001725

DE SCHEPPER, S., GROENEVELD, J., NAAFS, B. D. A., VAN RENTERGHEM, C., HENNISSEN, J., HEAD, M. J., LOUWYE, S. and FABIAN, K., 2013. Northern Hemisphere glaciation during the globally warm early Late Pliocene. *PloS One*, 8: e81508.

DE VERTEUIL, L. and NORRIS, G. 1996. Miocene dinoflagellate stratigraphy and systematics of Maryland and Virginia. Supplement. *Micropaleontology,* 42: 172p.

DOWSETT, H., 1991. The Development of a Long-Range Foraminifer Transfer Function and Application to Late Pleistocene North Atlantic Climatic Extremes. *Paleoceanography*, 6: 259–273, 10.1029/90PA02541

———, 2007. The PRISM palaeoclimate reconstruction and Pliocene sea-surface temperature. In: Williams, M., Haywood, A. M., Gregory, J., and Schmidt, D. N., Eds., *Deep-time perspectives on climate change: marrying the signal from computer models and biological proxies*, 459–480. London: The Geological Society. The Micropalaeontological Society, Special Publication.

DOWSETT, H. J., CHANDLER, M. A. and ROBINSON, M. M., 2009. Surface temperatures of the Mid-Pliocene North Atlantic Ocean: implications for future climate. *Philosophical Transactions of the Royal Society, A*, 367: 69–84, 10.1098/rsta.2008.0213

DOWSETT, H. J., CRONIN, T. M., POORE, R. Z., THOMPSON, R. S., WHATLEY, R. C. and WOOD, A. M., 1992. Micropaleontological Evidence for Increased Meridional Heat Transport in the North Atlantic Ocean During the Pliocene. *Science*, 258: 1133–1135, 10.1126/science.258.5085.1133

DOWSETT, H., DOLAN, A., ROWLEY, D., MOUCHA, R., FORTE, A. M., MITROVICA, J. X., POUND, M., SALZMANN, U., ROBINSON, M., CHANDLER, M., FOLEY, K. and HAYWOOD, A., 2016. The PRISM4 (mid-Piacenzian) paleoenvironmental reconstruction. *Climate of the Past*, 12: 1519–1538, 10.5194/cp-12-1519-2016

DOWSETT, H. J., FOLEY, K. M., ROBINSON, M. M. and HERBERT, T. D. 2017. PRISM late Pliocene (Piacenzian) alkenone - derived SST data. *U.S. Geological Survey Data Release*, https://doi.org/10.5066/F7959G1S

DOWSETT, H. J., FOLEY, K. M., STOLL, D. K., CHANDLER, M. A., SOHL, L. E., BENTSEN, M., OTTO-BLIESNER, B. L., BRAGG, F. J., CHAN, W.-L., CONTOUX, C., DOLAN, A. M., HAYWOOD, A. M., JONAS, J. A., JOST, A., KAMAE, Y., LOHMANN, G., LUNT, D. J., NISANCIOGLU, K. H., ABE-OUCHI, A., RAMSTEIN, G., RIESSELMAN, C. R., ROBINSON, M. M., ROSENBLOOM, N. A., SALZMANN, U., STEPANEK, C., STROTHER, S. L., UEDA, H., YAN, Q. and ZHANG, Z., 2013a. Sea Surface Temperature of the mid-Piacenzian Ocean: A Data-Model Comparison. *Scientific Reports* 3: 1-8, 10.1038/srep02013

DOWSETT, H.J. and POORE, R.Z., 1990. A new planktic foraminifer transfer function for estimating Pliocene—Holocene paleoceanographic conditions in the North Atlantic. *Marine Micropaleontology*, 16: 1–23. https://doi.org/10.1016/0377-8398(90)90026-I

———, 1991. Pliocene sea surface temperatures of the North Atlantic Ocean at 3.0 Ma. *Quaternary Science Reviews*, 10: 189–204, 10.1016/0277-3791(91)90018-P

DOWSETT, H. J. and ROBINSON, M. M., 2007. Mid-Pliocene planktic foraminifer assemblage of the North Atlantic Ocean. *Micropaleontology*, 53: 105–126. 10.2113/gsmicropal.53.1-2.105

———, 2016. A simple rubric for Stratigraphic Fidelity (β) of paleoenvironmental time series. *Stratigraphy*, 13: 303–305.

DOWSETT, H. J., ROBINSON, M. M., HAYWOOD, A. M., HILL, D. J., DOLAN, A. M., STOLL, D. K., CHAN, W.-L., ABE-OUCHI, A., CHANDLER, M. A., ROSENBLOOM, N. A., OTTO-BLIESNER, B. L., BRAGG, F. J., LUNT, D. J., FOLEY, K. M. and RIESSELMAN, C. R., 2012. Assessing confidence in Pliocene sea surface temperatures to evaluate predictive models. *Nature Climate Change*, 2: 365–371, 10.1038/NCLIMATE1455

DOWSETT, H., ROBINSON, M., HAYWOOD, A., SALZMANN, U., HILL, D., SOHL, L., CHANDLER, M., WILLIAMS, M., FOLEY, K. and STOLL, D., 2010. The PRISM3D paleoenvironmental reconstruction. *Stratigraphy*, 7: 123–139.

DOWSETT, H. J., ROBINSON, M. M., STOLL, D. K., FOLEY, K. M., JOHNSON, A. L. A., WILLIAMS, M. and RIESSELMAN, C. R., 2013b. The PRISM (Pliocene Palaeoclimate) reconstruction: Time for a paradigm shift. *Philosophical Transactions of the Royal Society*, 371: 1–24.

DOWSETT, H., THOMPSON, R., BARRON, J., CRONIN, T., FLEMING, F., ISHMAN, S., POORE, R., WILLARD, D. and HOLTZ JR, T., 1994. Joint investigations of the Middle Pliocene climate I: PRISM paleoenvironmental reconstructions. *Global and Planetary Change*, 9: 169–195, 10.1016/0921-8181(94)90015-9

DOWSETT, H. J. and WIGGS, L. B. 1992. Planktonic foraminiferal assemblage of the Yorktown Formation, Virginia, USA. *Micropaleontology,* 38: 75–86.

ELIAS, S. A. and MATTHEWS JR, J. V., 2002. Arctic North American seasonal temperatures from the latest Miocene to the Early Pleistocene, based upon mutual climatic range analysis of fossil beetle assemblages. *Canadian Journal of Earth Sciences*, 39: 911–920.

FENG, R., L. OTTO–BLIESNER, B., FLETCHER, T., TABOR, C., P. BALLANTYNE, A. and BRADY, E., 2017. Amplified Late Pliocene terrestrial warmth in northern high latitudes from greater radiative forcing and closed Arctic Ocean gateways. *Earth and Planetary Science Letters*, 466: 129-138, doi:10.1016/j.epsl.2017.03.006

FOLEY, K. M. and DOWSETT, H. J., 2019, Community sourced mid-Piacenzian sea surface temperature (SST) data. *U.S. Geological Survey data release*, https://doi.org/10.5066/P9YP3DTV.

GIBBARD, P. L., HEAD, M. J., WALKER, M. J. C. and THE SUBCOMMISSION ON QUATERNARY STRATIGRAPHY, 2010. Formal ratification of the Quaternary System/Period and the Pleistocene Series/Epoch with a base at 2.58 Ma. *Journal of Quaternary Science*, 25: 96–102, 10.1002/jqs.1338

GIBSON, T. G., 1983. Stratigraphy of Miocene through Lower Pleistocene strata of the United States central Atlantic coastal plain. In: Ray, C.E., RAY, Ed., *Geology and Paleontology of the Lee Creek Mine, North Carolina; I. Smithsonian Contributions to Paleobiology,* 53: 35–80.

GIDDEN, M. J., RIAHI, K., SMITH, S. J., FUJIMORI, S., LUDERER, G., KRIEGLER, E., VAN VUUREN, D. P., VANDEN BERG, M., FENG, L., KLEIN, D., CALVIN, K., DOELMAN, J. C., FRANK, S., FRICKO, O., HARMSEN, M., HASEGAWA, T., HAVLIK, P., HILAIRE, J., HOESLY, R., HORING, J., POPP, A., STEHFEST, E. and TAKAHASHI, K. 2019. Global emissions pathways under different socioeconomic scenarios for use in CMIP6: a dataset of harmonized emissions trajectories through the end of the century. *Geoscientific. Model Development*, 1212: 1443–1475, doi:10.5194/gmd-12-1443-2019, 2019.

GLADENKOV, Y. B., BARINOV, K., BASILIAN, A. and CRONIN, T., 1991. Stratigraphy and paleoceanography of Pliocene deposits of Karaginsky Island, eastern Kamchatka, USSR. *Quaternary Science Reviews*, 10: 239–245.

GROENEVELD, J., 2005. "Effect of the Pliocene closure of the Panamanian Gateway on Caribbean and east Pacific sea surface temperatures and salinities by applying combined Mg/Ca and $\delta^{18}O$ measurements (5.6–2.2 Ma)". Unpublished Ph.D. dissertation, University of Kiel, 165 pp.

HAUG, G. AND TIEDEMANN, R., 1998. Effect of the formation of the Isthmus of Panama on Atlantic Ocean thermohaline circulation. *Nature*, 393: 673–676, 10.1038/31447

HAUG, G., TIEDEMANN, R., ZAHN, R. and RAVELO, A., 2001. Role of Panama uplift on oceanic freshwater balance. *Geology*, 29: 207–210, 10.1130/0091-7613(2001)029<0207:ROPUOO>2.0.CO;2

HAYWOOD, A. M., DOLAN, A. M., PICKERING, S. J., DOWSETT, H. J., MCCLYMONT, E. L., PRESCOTT, C. L., SALZMANN, U., HILL, D. J., HUNTER, S. J. and LUNT, D. J. 2013a. On the identification of a Pliocene time slice for data–model comparison. *Philosophical Transactions of the Royal Society A*: Mathematical, Physical and Engineering Sciences, 371.

HAYWOOD, A. M., DOWSETT, H. J. and DOLAN, A. M. 2016a. Integrating geological archives and climate models for the mid-Pliocene warm period. *Nature Communications*, 7: 10646, 10.1038/ncomms10646

HAYWOOD, A. M., DOWSETT, H. J., DOLAN, A. M., ROWLEY, D., ABE-OUCHI, A., OTTO-BLIESNER, B., CHANDLER, M. A., HUNTER, S. J., LUNT, D. J., POUND, M. and SALZMANN, U. 2016b. The Pliocene Model Intercomparison Project (PlioMIP) Phase 2: scientific objectives and experimental design. *Climate of the Past*, 12: 663–675, 10.5194/cp-12-663-2016.

HAYWOOD, A. M., HILL, D. J., DOLAN, A. M., OTTO-BLIESNER, B. L., BRAGG, F., CHAN, W.-L., CHANDLER, M. A., CONTOUX, C., DOWSETT, H. J., JOST, A., KAMAE, Y., LOHMANN, G., LUNT, D. J., ABE-OUCHI, A., PICKERING, S. J., RAMSTEIN, G., ROSENBLOOM, N. A., SALZMANN, U., SOHL, L., STEPANEK, C., UEDA, H., YAN, Q. and ZHANG, Z. 2013b. Large-scale features of Pliocene climate: results from the Pliocene Model Intercomparison Project. *Climate of the Past*, 9: 191–209, 10.5194/cp-9-191-2013

HAZEL, J. E., 1971. Ostracode biostratigraphy of the Yorktown Formation (upper Miocene and lower Pliocene) of Virginia and North Carolina. *U.S. Geological Survey Professional Paper*, 704: 13pp.

HEMLEBEN, C., SPINDLER, M. and ANDERSON, O. R., 1989. *Modern Planktonic Foraminifera,* New York: Springer-Verlag, 363 pp.

HERBERT, T. D., 2001. Review of alkenone calibrations (culture, water column, and sediments). *Geochemistry Geophysics Geosystems*, 2: 1005, 10.1029/2000GC000055.

———, 2004. Alkenone palaeotemperature determinations. In: Elderfield, H., Holland, H. D. and Turekian, K. K., Eds., *The oceans and marine geochemistry*, Treatise on geochemistry: 391–432. Oxford: Elsevier-Pergamon.

HERBERT, T. D., CLEAVELAND PETERSON, L., LAWRENCE, K. T. and LIU, Z., 2010. Tropical ocean temperatures over the past 3.5 million years. *Science*, 328: 1530–1534, doi: 10.1126/science.1185435

HERBERT, T. D., NG, G. and PETERSON, L. C. 2015. Evolution of Mediterranean sea surface temperatures 3.5–1.5 Ma: regional and hemispheric influences. *Earth and Planetary Science Letters,* 409: 307–318.

HILBRECHT, H., 1996. Extant planktic foraminifera and the physical environment in the Atlantic and Indian Oceans, Mitteilungen aus dem Geologischen Institut der Eidgen. Technischen Hochschule und der Universität Zürich, Neue Folge. No. 300, 93pp. http://www.fuhrmann-hilbrecht.de/Heinz/geology/HH1996/aa_start.html

HODELL, D. A. and CHANNELL, J. E. T., 2016. Mode transitions in Northern Hemisphere glaciation: co-evolution of millennial and orbital variability in Quaternary climate. *Climate of the Past,* 12: 1805–1828, 10.5194/cp-12-1805-2016

HU, A., MEEHL, G. A., HAN, W., OTTO-BLIESTNER, B., ABE-OUCHI, A. and ROSENBLOOM, N., 2015. Effects of the Bering Strait closure on AMOC and global climate under different background climates. *Progress in Oceanography,* 132: 174–196, https://doi.org/10.1016/j.pocean.2014.02.004

HUANG, B., THORNE, P. W., BANZAN, V. F., BOYER, T., CHEPURIN, G., LAWRIMORE, J. H., MENNE, M. J., SMITH, T. M., VOSE, R. S. and ZHANG, H.-M., 2017. NOAA Extended Reconstructed Sea Surface Temperature (ERSST), Version 5. NOAA National Centers for Environmental Information. doi:10.7289/V5T72FNM (January 5, 2018).

HUNTER, S. J., HAYWOOD, A. M., DOLAN, A. M. and TINDALL, J. C. 2019. The HadCM3 contribution to PlioMIP Phase 2 Part 1: Core and Tier 1 experiments. *Climate of the Past Discussions,* 1–38. doi.org/10.5194/cp-2018-180

IMBRIE, J. and KIPP, N. G. 1971. A New Micropaleontological method for paleoclimatology: Application to a Late Pleistocene Caribbean core. In: Turekian, K. K., Ed., *The Late Cenozoic Glacial Ages*, 71–181. New Haven: Yale University Press.

IPCC, 2013: Climate Change 2013: The Physical Science Basis. Contribution of Working Group I to the Fifth Assessment Report of the Intergovernmental Panel on Climate Change. In: Stocker, T. F., D. Qin, G.-K. Plattner, M. Tignor, S. K. Allen, J. Boschung, A. Nauels, Y. Xia, V. Bex and P. M. Midgley, Eds., 1535pp. Cambridge: Cambridge University Press.

IVANOVA, E. V., BEAUFORT, L., VIDAL, L. and KUCERA, M., 2012. Precession forcing of productivity in the Eastern Equatorial Pacific during the last glacial cycle. *Quaternary Science Reviews*, 40: 64–77.

JOHNSON, A. L. A., VALENTINE, A., LENG, M. J., SLOANE, H., SCHONE, B.R. and BALSON, P. S., 2017. Isotopic Temperatures from the Early and Mid-Pliocene of the US Middle Atlantic Coastal Plain, and their implications for the cause of regional marine climate change. *Palaios*, 32: 250–269, doi:http://dx.doi.org/10.2110/palo.2016.080

KAMAE, Y., YOSHIDA, K. and UEDA, H., 2016. Sensitivity of Pliocene climate simulations in MRI-CGCM2.3 to respective boundary conditions. *Climate of the Past Discussions*, 2016: 1–29, 10.5194/cp-2016-50

KANDIANO, E. S., BAUCH, H. A. and MÜLLER, A., 2004. Sea surface temperature variability in the North Atlantic during the last two glacial–interglacial cycles: comparison of faunal, oxygen isotopic, and Mg/Ca-derived records. *Palaeogeography, Palaeoclimatology, Palaeoecology*, 204: 145–164, https://doi.org/10.1016/S0031-0182(03)00728-4

KARAS, C., NÜRNBERG, D., BAHR, A., GROENEVELD, J., HERRLE, J. O., TIEDEMANN, R. and DEMENOCAL, P. B., 2017. Pliocene oceanic seaways and global climate, *Scientific Reports*, 7: 39842, 10.1038/srep39842

KEIGWIN, L., 1982. Isotopic Paleoceanography of the Caribbean and East Pacific: Role of Panama Uplift in Late Neogene Time. *Science*, 217: 350–353, 10.1126/science.217.4557.350

KHELIFI, N., SARNTHEIN, M. and NAAFS, B. D. A., 2012. Technical note: Late Pliocene age control and composite depths at ODP Site 982, revisited. *Climate of the Past*, 8: 79–87, 10.5194/cp-8-79-2012

KRANTZ, D.E.,1991. A chronology of Pliocene sea-level fluctuations: The U.S. Middle Atlantic Coastal Plain record, *Quaternary Science Reviews,* 10: 163–174, doi: 10.1016/0277-3791(91)90016-N.

KÜRSCHNER, W. M., VAN DER BURGH, J., VISSCHER, H. and DILCHER, D. L. 1996. Oak leaves as biosensors of late neogene and early pleistocene paleoatmospheric CO_2 concentrations. *Marine Micropaleontology,* 27: 299–312, 0.1016/0377-8398(95)00067-4

LAWRENCE, K. T., HERBERT, T. D., BROWN, C. M., RAYMO, M. E. and HAYWOOD, A. M., 2009. High-amplitude variations in North Atlantic sea surface temperature during the early Pliocene warm period. *Paleoceanography*, 24: PA2218. 10.1029/2008pa001669

LAWRENCE, K. T., HERBERT, T. D., DEKENS, P. S. and RAVELO, A. C., 2007. The application of the alkenone organic proxy to the study of Plio-Pleistocene climate. In: Williams, M., Haywood, A. M., Gregory, F. J. and Schmidt, D. N., Eds., *Deep-time perspectives on climate change: marrying the signal from computer models and biological proxies*, Micropalaeontological Society (Special Publication), 539–562. London: Geological Society of London.

LISIECKI, L. E. and RAYMO, M. E., 2005. A Pliocene-Pleistocene stack of 57 globally distributed benthic $\delta^{18}O$ records. *Paleoceanography*, 20: 10.1029/2004PA001071

LOUBERE, P. and MOSS, K., 1986. Late Pliocene climatic change and the onset of Northern Hemisphere glaciation as recorded in the northeast Atlantic Ocean, *Geological Society of America Bulletin*, 97: 818–828, 10.1130/0016-7606(1986)97<818:LPCCAT>2.0.CO;2

LUNT, D., VALDES, P., HAYWOOD, A. and RUTT, I., 2008. Closure of the Panama Seaway during the Pliocene: implications for climate and Northern Hemisphere glaciation. *Climate Dynamics*, 30: 1–18, 10.1007/s00382-007-0265-6

MANSFIELD, W. C. 1943 [1944]. Stratigraphy of the Miocene of Virginia and the Miocene and Pliocene of North Carolina: Mollusca from the Miocene and lower Pliocene of Virginia and North Carolina: Part 1. Pelecypoda. With a summary of the stratigraphy. *U.S. Geological Survey Professional Paper,* 199-A:1-178. *With the publication of Professional Paper 199-B, a new cover and table of contents for parts A and B amended the issue date to January 1944.*

MARINCOVICH, L. and GLADENKOV, A. Y., 1999. Evidence for an early opening of the Bering Strait. *Nature*, 397: 149–151.

———, 2001. New evidence for the age of Bering Strait. *Quaternary Science Reviews*, 20: 329–335, 10.1016/S0277-3791(00)00113-X

MATTHIESSEN, J., KNIES, J., VOGT, C. and STEIN, R., 2009. Pliocene palaeoceanography of the Arctic Ocean and subarctic seas. *Philosophical Transactions of the Royal Society A: Mathematical, Physical and Engineering Sciences*, 367: 21–48, 10.1098/rsta.2008.0203

MÜLLER, P. J., KIRST, G., RUHLAND, G., VON STORCH, I., and ROSELL-MELE, A., 1998. Calibration of the alkenone paleotemperature index UK'37 based on core-tops from the eastern South Atlantic and the global ocean (60°N–60°S). *Geochimica et Cosmochimica Acta*, 62(10): 1757–1772.

NAAFS, B. D. A., HEFTER, J., ACTON, G., HAUG, G. H., MARTÍNEZ-GARCIA, A., PANCOST, R. and STEIN, R., 2012. Strengthening of North American dust sources during the late Pliocene (2.7 Ma). *Earth and Planetary Science Letters*, 317–318: 8–19, 10.1016/j.epsl.2011.11.026

NAAFS, B. D. A., STEIN, R., HEFTER, J., KHÈLIFI, N., DE SCHEPPER, S. and HAUG, G. H., 2010. Sea surface temperature (moving averages) versus time from IODP Site 306-U1313. In supplement to: Naafs, BDA et al. (2010): Late Pliocene changes in the North Atlantic Current. *Earth and Planetary Science Letters*, 298(3–4): 434–442, https://doi.org/10.1016/j.epsl.2010.08.023

O'BRIEN, C. L., FOSTER, G. L., MARTÍNEZ-BOTÍ, M. A., ABELL, A., RAE, J. W. and PANCOST, R. D., 2014. High sea surface temperatures in tropical warm pools during the Pliocene. *Nature Geoscience*, 7: 606–611, doi: 10.1038/NGEO2194

O'DEA, A., LESSIOS, H. A., COATES, A. G., EYTAN, R. I., RESTREPO-MORENO, S. A., CIONE, A. L., COLLINS, L. S., DE QUEIROZ, A., FARRIS, D. W., NORRIS, R. D., STALLARD, R. F., WOODBURNE, M. O., AGUILERA, O., AUBRY, M.-P., BERGGREN, W. A., BUDD, A. F., COZZUOL, M. A., COPPARD, S. E., DUQUE-CARO, H., FINNEGAN, S., GASPARINI, G. M., GROSSMAN, E. L., JOHNSON, K. G., KEIGWIN, L. D., KNOWLTON, N., LEIGH, E. G., LEONARD-PINGEL, J. S., MARKO, P. B., PYENSON, N. D., RACHELLO-DOLMEN, P. G., SOIBELZON, E., SOIBELZON, L., TODD, J. A., VERMEIJ, G. J. and JACKSON, J. B. C., 2016. Formation of the Isthmus of Panama. *Science Advances*, 2(8): e1600883, 10.1126/sciadv.1600883

OGG, J. G., 2012. Chapter 5 - Geomagnetic Polarity Time Scale. *The Geologic Time Scale*, 85–113. Boston: Elsevier.

OPPO, D. W. and FAIRBANKS, R. G. 1987. Variability in the deep and intermediate water circulation of the Atlantic Ocean during the past 25,000 years: Northern Hemisphere modulation of the Southern Ocean. *Earth and Planetary Science Letters,* 86: 1–15.

OTTO-BLIESNER, B., JAHN, A., FENG, R., BRADY, E., HU, A. and LÖFVERSTRÖM, M. 2017. Changes in Arctic Gateways Amplify North Atlantic Warming in the Late Pliocene: Arctic Gateways and Pliocene Climate. *Geophysical Research Letters*, 44: 957–964. 10.1002/2016GL071805

PAGANI, M., LIU, Z., LARIVIERE, J. and RAVELO, A. C. 2010. High Earth-system climate sensitivity determined from Pliocene carbon dioxide concentrations. *Nature Geoscience,* 3: 27–30, 10.1038/ngeo724

PANITZ, S., SALZMANN, U., RISEBROBAKKEN, B., DE SCHEPPER, S. and POUND, M. J., 2016. Climate variability and long-term expansion of peat lands in Arctic Norway during the late

Pliocene (ODP Site 642, Norwegian Sea). *Climate of the Past*, 12: 1043–1060, doi:10.5194/cp-12-1043-2016

PANITZ, S., SALZMANN, U., RISEBROBAKKEN, B., DE SCHEPPER, S., POUND, M. J., HAYWOOD, A. M., DOLAN, A. M. and LUNT, D. J., 2018. Orbital, tectonic and oceanographic controls on Pliocene climate and atmospheric circulation in Arctic Norway. *Global and Planetary Change*, 161: 183–193, https://doi.org/10.1016/j.gloplacha.2017.12.022

PARKER, F. L., 1962. Planktonic foraminiferal species in Pacific sediments, *Micropaleontology*, 8: 219–254, 10.2307/1484745.

———, 1967. Late Tertiary biostratigraphy (planktonic foraminifera) of tropical Indo-Pacific deep-sea cores, *Bulletin of American Paleontology*, 52: 115–208.

POORE, H. R., SAMWORTH, R., WHITE, N. J., JONES, S. M. and MCCAVE, I. N., 2006. Neogene overflow of Northern Component Water at the Greenland-Scotland Ridge. *Geochemistry, Geophysics, Geosystems,* 7: Q06010, doi: 10.1029/2005GC001085

PRELL, W., MARTIN, A., CULLEN, J. and TREND, M., 1999. Brown University Foraminiferal Database, *NOAA, https://www.ncdc.noaa.gov/paleo-search/study/5908.*

PRESCOTT, C.L., HAYWOOD, A.M., DOLAN, A.M., HUNTER, S.J., POPE, J.O. and PICKERING, S.J., 2014. Assessing orbitally-forced interglacial climate variability during the mid-Pliocene warm period. *Earth and Planetary Science Letters*, 400:261–271.

RAVELO, A. C., FAIRBANKS, R. G. and PHILANDER, G., 1990. Resconstructing tropical Atlantic hydrography using planktonic foraminifera and an ocean model. *Paleoceanography*, 5: 409–431, https://doi.org/10.1029/PA005i003p00409

RAYMO, M. E., GRANT, B., HOROWITZ, M. and RAU, G. H. 1996. Mid-Pliocene warmth: stronger greenhouse and stronger conveyor. *Marine Micropaleontology,* 27: 313–326, 10.1016/0377-8398(95)00048-8

REBOTIM, A., VOELKER, A. H. L., JONKERS, L., WANIEK, J. J., MEGGERS, H., SCHIEBEL, R., FRAILE, I., SCHULZ, M. and KUCERA, M., 2017. Factors controlling the depth habitat of planktonic foraminifera in the subtropical eastern North Atlantic. *Biogeosciences,* 14: 827–859, doi.org/10.5194/bg-14-827-2017

RIND, D. and CHANDLER, M.A., 1991. Increased ocean heat transports and warmer climate. *Journal of Geophysical Research*, 96: 7437–7461, 10.1029/91JD00009

RISEBROBAKKEN, B., ANDERSSON, C., DE SCHEPPER, S. and MCCLYMONT, E.L. 2016. Low-frequency Pliocene climate variability in the eastern Nordic seas. *Paleoceanography*, 31: 1154–1175.

ROBINSON, M. M., DOWSETT, H. J., DWYER, G. S. and LAWRENCE, K. T., 2008. Reevaluation of mid-Pliocene North Atlantic sea surface temperatures. *Paleoceanography,* 23: PA3213, doi:10.1029/2008PA001608

ROBINSON, M. M., DOWSETT, H. J., FOLEY, K. M. and RIESSELMAN, C. R. 2018. PRISM marine sites—The history of PRISM sea surface temperature estimation. *U. S. Geological Survey Open-File Report* 2018–1148, 49 pp., https://doi.org/10.3133/ofr20181148.

ROBINSON, M., FOLEY, K., DOWSETT, H. and SPIVEY, W., 2019. A global planktic foraminifer census data set for the Pliocene ocean, addendum. NOAA National Centers for Environmental Information, https://www.ncdc.noaa.gov/paleo/study/27310.

ROBINSON, M. M., VALDES, P. J., HAYWOOD, A. M., DOWSETT, H. J., HILL, D. J. and JONES, S. M. 2011. Bathymetric controls on Pliocene North Atlantic and Arctic sea surface temperature and deep-water production. *Palaeogeography, Palaeoclimatology, Palaeoecology,* 309: 92–97.

ROGELJ, J., POPP, A., CALVIN, K.V., LUDERER, G., EMMERLING, J., GERNAAT, D., FUJIMORI, S., STREFLER, J., HASEGAWA, T., MARANGONI, G., KREY, V., KRIEGLER, E., RIAHI, K., VAN VUUREN, D.P., DOELMAN, J., DROUET, L., EDMONDS, J., FRICKO, O., HARMSEN, M., HAVLIK, P., HUMPENÖDER, F., STEHFEST, E. and TAVONI, M. 2018. Scenarios towards limiting global mean temperature increase below 1.5 °C. *Nature Climate Change,* 8(2018): 325–332, doi:10.1038/s41558-018-0091-3

ROSENBLOOM, N. A., OTTO-BLIESNER, B. L., BRADY, E.C. and LAWRENCE, P. J., 2013. Simulating the mid-Pliocene Warm Period with the CCSM4 model, Geoscientific Model Development, 6(2): 549–561, doi:10.5194/gmd-6-549-2013.

ROWLEY, D. B., FORTE, A. M., MOUCHA, R., MITROVICA, J. X., SIMMONS, N. A. and GRAND, S. P., 2013. Dynamic Topography Change of the Eastern United States Since 3 Million Years Ago. *Science*, 340: 1560–1563, 10.1126/science.1229180

SALZMANN, U., DOLAN, A. M., HAYWOOD, A. M., CHAN, W.-L., VOSS, J., HILL, D. J., ABE-OUCHI, A., OTTO-BLIESNER, B., BRAGG, F. J., CHANDLER, M. A., CONTOUX, C., DOWSETT, H. J., JOST, A., KAMAE, Y., LOHMANN, G., LUNT, D. J., PICKERING, S. J., POUND, M. J., RAMSTEIN, G., ROSENBLOOM, N. A., SOHL, L., STEPANEK, C., UEDA, H. and ZHANG, Z. 2013. Challenges in quantifying Pliocene terrestrial warming revealed by data–model discord. *Nature Climate Change*, 3: 969–974, 10.1038/nclimate2008

SALZMANN, U., HAYWOOD, A.M., LUNT, D.J., VALDES, P.J. and HILL, D. J., 2008. A new global biome reconstruction and data-model comparison for the middle Pliocene. *Global Ecology and Biogeography,* 17: 432–447.

SARNTHEIN, M., BARTOLI, G., PRANGE, M., SCHMITTNER, A., SCHNEIDER, B., WEINELT, M., ANDERSEN, N. and GARBE-SCHÖNBERG, D., 2009. Mid-Pliocene shifts in ocean overturning circulation and the onset of Quaternary-style climates. *Climate of the Past*, 5: 269–283, 10.5194/cp-5-269-2009

SAUPE, E. E., HENDRICKS, J. R., PORTELL, R. W., DOWSETT, H. J., HAYWOOD, A. M., HUNTER, S. J. and LIEBER MAN, B. S., 2014. Macroevolutionary consequences of profound climate change on niche evolution in marine molluscs over the past three million years. *Proceedings of the Royal Society B*: Biological Sciences, 281: 20141995, http://dx.doi.org/10.1098/rspb.2014.1995

SEKI, O., FOSTER, G. L., SCHMIDT, D. N., MACKENSEN, A., KAWAMURA, K. and PANCOST, R. D. 2010. Alkenone and boron-based Pliocene pCO2 records. *Earth and Planetary Science Letters,* 292: 201–211, 10.1016/j.epsl.2010.01.037

SHANNON, C. E., 1948. A mathematical theory of communication. *The Bell System Technical Journal*, 27: 379–423, 10.1002/j.1538-7305.1948.tb01338.x

SHIPBOARD SCIENTIFIC PARTY, 1996. Site 982. *Proceedings of the Ocean Drilling Program Initial Reports*, 162: 91–138.

SNYDER, S. W., MAUGER, L. L. and AKERS, W. H., 1983. Planktonic foraminifera and biostratigraphy of the Yorktown Formation, Lee Creek Mine. In: Ray, C. E., Ed., *Geology and Paleontology of the Lee Creek Mine, North Carolina, I.* Smithsonian Contributions to Paleobiology, 53: 455–481.

SOHL, L. E., CHANDLER, M. A., SCHMUNK, R. B., MANKOFF, K., JONAS, J. A., FOLEY, K. M. and DOWSETT, H. J. 2009. PRISM3/GISS topographic reconstruction. *U. S. Geological Survey Data Series* 419:1–6, http://pubs.usgs.gov/ds/419/

SPIEGLER, D. and JANSEN, E., 1989. Planktonic foraminifer biostratigraphy of Norwegian Sea sediments: ODP Leg 104. *Ocean Drilling Program, Scientific Results,* 104: 681–696.

STEPH, S., TIEDEMANN, R., PRANGE, M., GROENEVELD, J., NÜRNBERG, D., REUNING, L., SCHULZ, M. and HAUG, G. H., 2006. Changes in Caribbean surface hydrography during the Pliocene shoaling of the Central American Seaway. *Paleoceanography*, 21: PA4221, 10.1029/2004PA001092

THOMPSON, R. S. and FLEMING, R. F., 1996. Middle Pliocene vegetation: reconstructions, paleoclimatic inferences, and boundary conditions for climate modeling. *Marine Micropaleontology*, 27: 27–49, 10.1016/0377-8398(95)00051-8

TZANOVA, A. and HERBERT, T. D. 2015. Regional and global significance of Pliocene sea surface temperatures from the Gulf of Cadiz (Site U1387) and the Mediterranean. *Global and Planetary Change,* 133: 371–377, doi:https://doi.org/10.1016/j.gloplacha.2015.07.001

VERHOEVEN, K., LOUWYE, S., EIRÍKSSON, J. and DE SCHEPPER, S., 2011. A new age model for the Pliocene–Pleistocene Tjörnes section on Iceland: Its implication for the timing of North Atlantic–Pacific palaeoceanographic pathways. *Palaeogeography, Palaeoclimatology, Palaeoecology,* 309: 33–52.

VOLKMAN, J. K., 2000. Ecological and environmental factors affecting alkenone distributions in seawater and sediments. *Geochemistry, Geophysics, Geosystems,* 1: 1036, doi: 10.1029/2000GC000061

WARD, L. W. and BLACKWELDER, B. W., 1980. Stratigraphic revision of upper Miocene and lower Pliocene beds of the Chesapeake Group, Middle Atlantic coastal plain. *U.S. Geological Survey Bulletin*, *1482-D*, 61pp.

WARD L. W., BAILEY R. H. and CARTER J. G., 1991. Pliocene and early Pleistocene stratigraphy, depositional history, and molluscan paleobiogeography of the Coastal Plain. In: Horton, J. W. Jr., and Zullo V. A., Eds., *The Geology of the Carolinas*, 274–289. Knoxville: University of Tennessee Press.

WEAVER, P. P. E., 1986. Late Miocene-Recent planktonic foraminifers from the North Atlantic: Deep sea drilling project leg 94. *Initial Reports of the Deep Sea Drilling Project,* 94:703–727.

WILLARD, D. A. 1994. Palynological record from the North Atlantic region at 3 Ma: vegetational distribution during a period of global warmth. *Review of Palaeobotany and Palynology*, 83: 275–297. 10.1016/0034-6667(94)90141-4

WILLARD, D. A. 1996. Pliocene-Pleistocene pollen assemblages from the Yermak Plateau, Arctic Ocean, Sites 910 and 911. *Proceedings of the Ocean Drilling Program, Scientific Results*, 151: 297–305, 10.2973/odp.proc.sr.151.115

WRIGHT, J. D. and MILLER, K. G. 1996. Control of North Atlantic Deep Water Circulation by the Greenland-Scotland Ridge. *Paleoceanography,* 11: 157–170.

WUEBBLES, D. J., FAHEY, D. W., HIBBARD, K. A., DOKKEN, D. J., STEWART, B. C. and MAYCOCK, T. K., 2017. *Climate Science Special Report: Fourth National Climate Assessment, Volume I.* Washington, DC: U.S. Global Change Research Program, 470 pp, doi: 10.7930/J0J964J6.

YASUHARA, M., HUNT, G., DOWSETT, H. J., ROBINSON, M. M. and STOLL, D. K. 2012. Latitudinal species diversity gradient of marine zooplankton for the last three million years. *Ecology Letters*, 15: 1174–1179, 10.1111/j.1461-0248.2012.01828.x

ZHANG, Z. S., NISANCIOGLU, K. H., CHANDLER, M. A., HAYWOOD, A. M., OTTO-BLIESNER, B. L., RAMSTEIN, G., STEPANEK, C., ABE-OUCHI, A., CHAN, W. L., BRAGG, F. J., CONTOUX, C., DOLAN, A. M., HILL, D. J., JOST, A., KAMAE, Y., LOHMANN, G., LUNT, D. J., ROSENBLOOM, N. A., SOHL, L. E. and UEDA, H., 2013. Mid-Pliocene Atlantic Meridional Overturning Circulation not unlike modern. *Climate of the Past*, 9: 1495–1504, 10.5194/cp-9-1495-2013

ZHENG, J., ZHANG, Q., LI, Q., ZHANG, Q. and CAI, M., 2018. Contribution of sea-ice albedo and insulation effects to Arctic amplification in the EC-Earth Pliocene simulation. *Climate of the Past Discussions*, https://doi.org/10.5194/cp-2018–59.

ZUBAKOV, V. A. and BORZENKOVA, I. I., 1988. Pliocene palaeoclimates: Past climates as possible analogues of mid-twenty-first century climate. *Palaeogeography, Palaeoclimatology, Palaeoecology*, 65: 35–49 10.1016/0031-0182(88)90110-1

APPENDIX 1

Supplementary information.

Ecogroups

Ecogroup categories 1, 2, 3 and 4, modified from Aze et al. (2011), were used to construct text-figure 6. Groups 1 and 2 were combined into a single mixed layer group. Group 5 representing high latitude taxa was not plotted.

1. (**mixed layer symbiotic**): *Dentoglobigerina altispira, Globigerina eamesi, Gobigerina falconensis, Globigerina umbilicata, Globigerinoides conglobatus, Globigerinoides extremus, Globigerinoides fistulosus, Globigerinoides obliquus, Globigerinoides ruber, Globigerinoides sacculifer, Globigerina woodi*

2. (**mixed layer asymbiotic**): *Globigerina bulloides, Globigerina apertura, Globigerina decoraperta, Globigerina nepenthes, Globigerina rubescens*

3. (**thermocline**): *Dentoglobigerina baroemoenensis, Dentoglobigerina globosa, Globigerinella calida, Globigerinella obesa, Globorotalia inflata, Globorotalia puncticulata, Globoquadrina conglomerata, Globorotalia flexuosa, Globorotalia tumida, Globorotalia ungulata, Globorotalia menardii, Globorotalia multicamerata, Neogloboquadrina acostaensis, Neogloboquadrina dutertrei, Neogloboquadrina humerosa, Pulleniatina obliquiloculata, Sphaeroidinella dehiscens, Sphaeroidinellopsis seminulina, Globigerina pseudobesa, Globigerinella aequilateralis*

4. (**subthermocline**): *Globigerina digitata, Globigerina praedigitata, Globorotaloides hexagona, Globorotalia hirsuta, Globorotalia scitula, Globorotalia theyeri, Orbulina universa, Globorotalia crassaformis, Globorotalia crassula, Globorotalia tosaensis, Globorotalia truncatulinoides*

5. (**high latitude**): *Turborotalita quinqueloba, Globigerinita glutinata, Neogloboquadrina pachyderma, Neogloboquadrina incompta*

SST anomalies for data-model comparisons

Data

Piacenzian SST anomalies [ΔSST_{plio}] are calculated by subtracting the pre-industrial (PI) mean annual SST [SST_{pi}] from the mean of the n U^k_{37} SST estimates falling between 3.210 Ma and 3.200 Ma at each site [SST_{plio}]. Table 1 in the text provides SST_{pi} , SST_{plio} , ΔSST_{plio}, n and σ for each locality.

SST_{pi} is the mean annual SST at each site from the years 1870-1899 (to avoid modern global warming) in the NOAA Extended Reconstructed SST.v5 (Huang et al. 2017).

We calculate uncertainty for ΔSST_{plio} as

$$\sqrt{((\sigma SST_{plio})^2 + (\sigma SST_{pi})^2)}$$

Model

CCSM4 Piacenzian SST anomalies [ΔSST_{model}] are calculated by subtracting the model control run SST [SST_{ctrl}] from the SST_{model} at each site. SST_{model} is the average of the 100 mean annual SST's representing the last 100 years of the simulation. Table 1 in the text provides ΔSST_{model} and sigma for each locality.

We calculate uncertainty for ΔSST_{model} as

$$\sqrt{((\sigma SST_{model})^2 + (\sigma SST_{ctrl})^2)}$$

Model and Experimental Design

Otto-Bliesner et al. (2017) reported on Pliocene coupled climate simulations using the Community Climate System Model version 4 (CCSM4). Details of the model can be found in Otto-Bliesner et al. (2017) and Rosenbloom et al. (2013). The PlioMIP1 simulation used atmospheric CO_2 set to 405 ppmv (parts per million by volume; Kurschner et al. (1996), Raymo et al. (1996), Pagani et al. (2010), Seki et al. (2010)) and PRISM3 boundary conditions (Dowsett et al. 2010; Rosenbloom et al. 2013). The positions of continents and distribution of land and sea (land-sea mask) is modern except for filling in of Hudson Bay as land.

Sensitivity experiments included a PI simulation using conditions for 1850, a simulation with only the Bering Strait closed, another with only the Canadian Arctic Archipelago closed, and a third with both gateways closed. This third simulation is most like the PRISM4 boundary conditions being used in PlioMIP2 (Dowsett et al. 2016; Haywood et al. 2016).

Seasonality

Seasonality is estimated as the difference between winter [SST_{feb}] and summer [SST_{aug}]:

$$\text{SEASONALITY} = SST_{aug} - SST_{feb}$$

with estimates for SST_{aug} and SST_{feb} calculated using transfer function GSF18 (Dowsett and Poore 1990; Dowsett 1991) on faunal assemblage data found in Robinson et al. (2019).

Holland Core (DEQ161-592) Information

Corehole:	Holland Rotosonic DEQ161-592
County/State:	City of Suffolk, Virginia
Start Date:	October 2, 2012
End Date:	October 4, 2012
Total Depth:	456 ft
Geologist:	T. Scott Bruce
Land Surface:	78.583 ft elevation NAVD88
Latitude:	36°40' 55.57990" DMS NAD 83
Longitude:	76°46' 50.0909044" DMS NAD 83
Well logs:	Gamma Ray, Resistivity
Archive:	U.S. Geological Survey, Reston Virginia
Paleontology:	Sampled for foraminifera, dinoflagellates, nannofossils, spores and pollen

APPENDIX TABLE 1
Sesonality estimates.

1313		662		981		1308		999	
Age (ka)	Seasonality (°C)	Age (ka)	Seasonality (°C)	Age (ka)	Seasonality (°C)	Age (ka)	Seasonality (°C)	Age (ka)	Seasonality (°C)
3191.57	8.8	3198.81	5.2	3233.67	3.5	3161.88	5.9	3198.40	3.7
3192.76	8.9	3207.21	6.2	3233.89	3.7	3163.60	7.5	3201.60	3.4
3194.77	8.0	3209.84	0.6	3234.10	3.4	3165.33	7.6	3204.80	3.4
3197.70	7.2	3212.27	4.9	3234.30	4.0	3167.06	7.9	3208.20	2.7
3201.07	7.7	3214.38	5.8	3234.50	3.4	3168.79	6.9	3211.60	3.8
3203.74	8.2	3216.49	6.5	3234.50	0.0	3170.51	8.0	3215.00	5.2
3208.72	7.8	3218.59	6.6	3234.73	3.7	3172.24	5.7	3218.40	3.5
3213.68	7.0	3220.69	5.8	3234.95	5.6	3176.18	5.9	3221.80	6.2
3217.48	5.8	3222.78	7.0	3235.38	6.6	3180.53	6.3	3225.20	3.2
3220.96	6.1	3224.43	6.5	3235.80	4.0	3184.90	8.1	3228.60	2.5
3224.17	6.8	3226.61	5.8	3236.02	3.5	3189.26	6.2	3232.00	2.9
3229.88	7.8	3229.06	5.2	3236.23	3.6	3193.63	7.6	3235.40	3.1
3237.20	4.2	3230.87	4.9	3236.44	3.7	3197.99	6.8	3238.80	4.3
3246.44	6.0	3233.26	6.7	3236.65	3.6	3202.36	8.1	3242.20	4.6
3258.63	6.1	3235.75	6.1	3236.87	3.7	3206.72	8.0	3245.60	3.8
3271.71	5.8	3238.52	6.4	3237.08	2.9	3212.54	8.1	3249.00	3.4
3282.09	6.7	3242.15	6.7	3237.30	3.5	3216.91	8.2	3252.40	2.3
3282.09	7.2	3247.31	6.1	3237.51	3.4	3221.27	8.1	3255.60	2.3
3285.70	6.4	3257.28	4.5	3237.72	3.6	3230.73	8.4	3258.90	3.6
3293.28	6.7	3266.64	5.0	3237.93	3.5	3235.82	8.6	3262.30	2.9
3298.71	6.7	3275.63	4.9	3238.15	3.5	3240.19	7.8	3265.70	4
3302.96	2.9	3286.69	5.1	3238.36	3.6	3244.55	7.6	3269.10	4.1
3305.97	4.4	3295.89	6.7	3238.58	3.5	3248.92	7.6	3272.50	2.7
3307.98	3.9	3304.45	3.3	3238.79	3.5	3253.28	6.3	3279.30	2.8
3309.99	3.7	3319.63	4.7	3238.79	0.0	3257.65	7.2	3282.70	2.9
3312.95	3.2	3331.80	6.9	3239.00	3.5	3261.83	7.2	3286.10	2.6
3316.10	3.1			3239.21	3.5	3265.31	7.2	3289.50	2.7
3318.81	3.5			3239.43	3.5	3268.33	5.9	3292.90	1.6
3321.10	2.8			3239.65	3.8	3271.28	6.2	3296.20	1
				3239.86	3.7	3274.44	6.4	3299.60	2.8
				3240.07	3.7	3277.71	7.6	3302.70	2.2
				3240.28	3.7	3280.86	5.8	3305.50	1.6
				3240.49	3.7	3284.23	7.6	3308.10	1.1
						3288.02	7.4	3312.40	1.3
						3292.22	7.9		
						3296.86	7.7		
						3301.20	6.9		